M. Sc. Sustainable Materials

Polymer Sciences

Macromolecular Chemistry

Lab Course

-- Theory --

„Willst du etwas wissen, so frage einen Erfahrenen und keinen Gelehrten.“

Chinesisches Sprichwort

Impressum

Dieses Skript ist im Wintersemester 2014/15 am Institut für Makromolekulare Chemie der Albert-Ludwigs-Universität Freiburg entstanden.

Im Wintersemester 2019/20 wurde das Skript überarbeitet und aktualisiert.

Einige der enthaltenen Kapitel basieren auf früheren Skripten aus dem Institut, die aktualisiert, angepasst und übersetzt wurden. Einige Kapitel sind völlig neu entstanden.

Es waren die folgenden Autoren beteiligt: Benjamin S. Ritter, Daniel Vonwil, Markus Heiny, Maziar Matloubi, Stephan Laule, Ralf Hanselmann und Michael Sommer.

Titelbild: Vitalij Schimpf

Table of Content

1. General annotations

In this lab course various core issues of polymer chemistry will be taught. Each experiment contains the basic components polymerization, polymer analysis, processing, and morphology characterization. As these core competences are exemplified by bio-based and biodegradable (co)polymers, the student is simultaneously introduced into the fields of sustainable materials and general concepts and principles of polymer chemistry. In the preparative part one will deal with different syntheses of bio-based and biodegradable polylactide. Polycaprolactone which is a crude oil-based but biodegradable polymer will be synthesized, too. Ring-opening polymerization is an effective way to synthesize polymers. Therefore the two aforementioned examples are implemented in this course. In the field of analysis one will analyze the composition and the molecular weight (distribution) using three core methods of polymer analysis (NMR, SEC and MALDI-TOF). Thermal analysis using DSC and TGA is another important aspect in this internship and in polymer science. For investigating the mechanical properties of the synthesized polymers, different ways of polymer processing are performed in the practical. Working with a mini compounder, injection molding, melt pressing and electro-spinning; different important processing methods are introduced. Rheological experiments as well as morphology investigations will complete the practical.

1.1 Prerequisites

In order to being admitted for this lab course, an examination has to be passed. Times of the examinations will be communicated.

While this script contains the most important theoretical background for this lab course, further reading may be required in some instances. More comprehensive literature is given at the end of each section.

The safety concerns of the experiment must be assessed before the start of the practical work. **A safety and operating instruction form has to be prepared for the experiments and signed by the supervisor.** Details for preparation and handing in of the forms will be communicated by the supervisor.

1.2 Lab Journal and Protocol

The students have to document all procedures (experiments, analysis etc.) carried out during the lab course in a **lab journal** (a **bound** notebook without the possibility to remove pages; i.e. spiral-bound notepads and the like are not allowed).

Furthermore, each group has to hand in a protocol covering the work done in this lab course. The protocol should include a compact theoretical part as well as the presentation and discussion of the synthetic and analytical work. The specific requirements will be communicated by the supervisors. The protocol has to be submitted until the date and time stated below.

General requirements:

- Justification ("Blocksatz")
- Font size: 10 - 12
- 1.25-line spacing
- All figures and tables have to be labeled and referred to in the text.
- Research in online sources is of course useful and necessary. Naturally, copy-and-pasting of text passages is no option and every source used to writing the protocol has to be properly cited. Likewise, copying from old protocols is prohibited. Being uncovered in 95 % of all cases, copy-and-pasting leads to failing of the lab course. In severe cases, university administration will be involved and exmatriculation may be a consequence.

1.3 Lab Safety

For carrying out the experiments, a lab coat and safety glasses must be worn at all times in lab. It is the students' responsibility to have these items ready at the beginning of the lab course. In addition to wearing a lab coat and safety glasses, closed shoes and long pants must be worn during all times in the lab. Any lab work or experimental procedure may only begin after all security-related issues have been clarified and a safety briefing has been done. In all safety-related matters, the supervisors' instructions have to be followed. More safety rules will be announced in the general safety instruction seminar before the lab course starts.

2. Concepts of Green Chemistry and Green Polymerization

In Principle 1 of the "Rio Declaration on Environment and Development" from June 1992 it is announced that human beings are the center of concerns for sustainable development and that they are entitled to a healthy and productive life in harmony with nature.[1] This early statement underlines the necessity of a change in global industry and our daily life to a more sustainable behavior and production of goods to "live in harmony with nature". Our daily impressions from global warming caused by greenhouse gas emissions and the diminishing fossil fuels force scientists to think about alternatives to existing industrial production processes and to make the established procedures much more efficient. A common definition of a sustainable development is that it must meet the needs of the present generation without compromising those of future ones.[2] Chemistry has a strong responsibility to contribute to a sustainable development. The principles of Green Chemistry as pointed out by P. T. Anastas and J. Warner from US-EPA are meanwhile spread widely. The 12 principles of Green Chemistry are show in **Figure 1**.

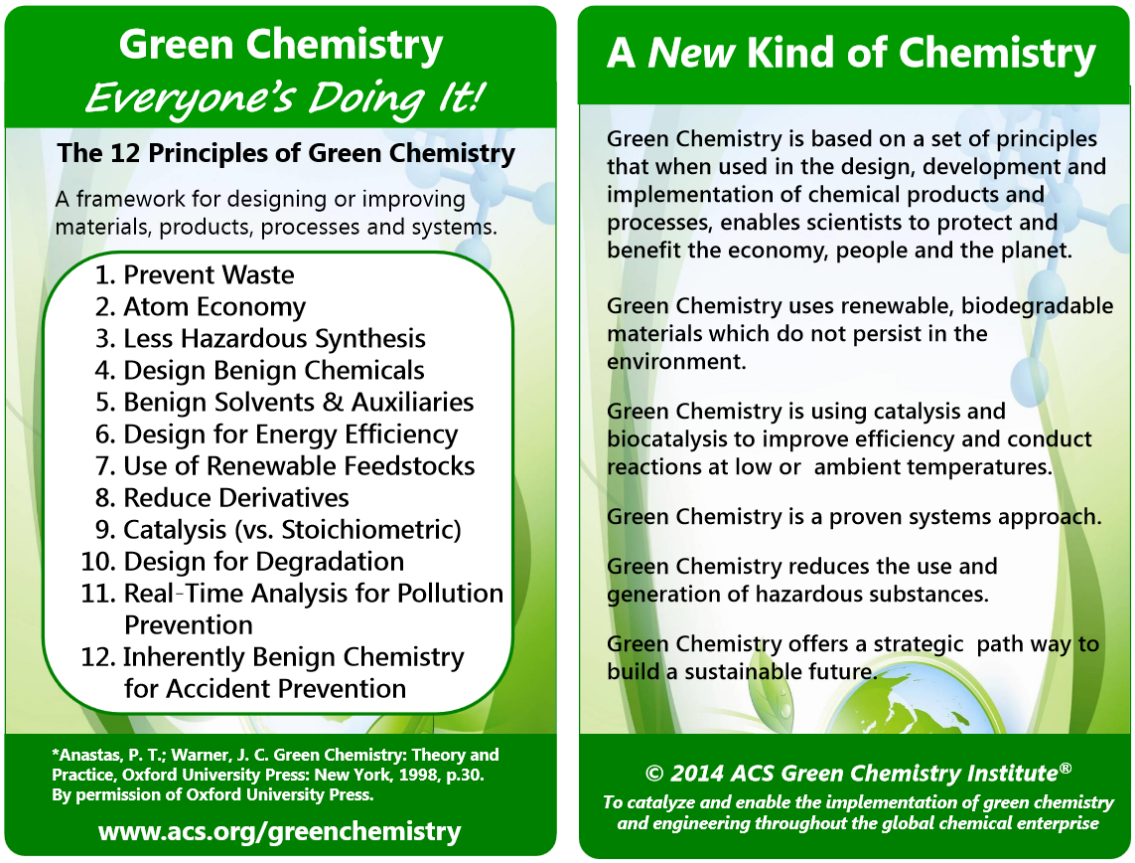

Figure 1: The 12 principles of Green Chemistry announced by Anastas and Warner.

The production and use of polymers increases from year to year and will reach 300 Mio. tons per year in less than a decade. Thus, polymer chemistry offers an enormous potential to implement Green Chemistry into production and processing to make products with less toxicity, biodegradability and better biocompatibility. By using bio-based raw materials for polymer production other property profiles can be generated. Via so-called drop-in processes (synthesizing the known and already used monomers via a green route and working with the existing polymerization reactors, processing machinery and distribution chains) a cheap solution is found to shift polymer synthesis from oil to bio-based resources.

However, a lot of information about sustainability is available which needs to be checked carefully. Some innovations were just motivated by greenwashing and covering up real problems. Greenwashing and the debate about the competition between dinner plates and fuel tanks (e.g. Mexico´s Tortilla Crisis from 2007[1]) clearly show that generalization should not be done in this field and that a careful case-by-case evaluation is necessary here.

Nevertheless, the 12 principles of Green Chemistry can be easily checked experimentally for a special reaction by scientific methods in order to evaluate its benefit toward sustainability without raising unnecessarily extensive discussions about the results. A more complicated case is to valuate numbers in complex and interconnected industrial processes. Here, it is important that the source of data is trustworthy.

In green polymerization the importance of catalysis must not be underestimated. Since Karl Ziegler and Giulio Natta received the Nobel Prize in 1963, catalytic syntheses of polyolefins have gained increasing importance. Other Noble Prizes were awarded to scientists working on catalysis in 2001(Knowles, Noyori, Sharpless) and 2005 (Chauvin, Grubbs, Schrock). For industrial processes, catalysis is just as important as in the academic world. Moreover, organocatalysts and biocatalysts have emerged as complementary methods to traditional transition-metal-based catalysts. The efficiency of a catalyst is usually measured as turnover numbers (TONs) or as catalyst activity (kg polymer/ mol catalyst · h). For green reactions the E-factor, quantifying the amount of waste produced during a process compared with the quantity of the desired product, is a more accurate parameter that should be considered.[3]

The ideal E-factor equals zero, but many reactions do not result in 100 % conversion, show side reactions, require solvents, and so on. Another measurement system to judge on a reaction with respect to sustainability is the hands-on EcoScale.[4] In this concept, penalty points are given to the chemical reaction, the work-up, the synthesis method and so on.

Green polymers are based on a broad range of renewable resources such as lignin, triglycerides, polysaccharides, monoterpenes, furans, lactides and natural rubber. Renewable resources can also be used for sustainable reaction conditions to reduce waste or eliminate volatile organic solvents. In this context, biodiesel is a very useful polymerization solvent for free-radical polymerization and a great alternative to conventional petroleum based solvents.[5]

Bibliography and Further Readings:

[1]USA started to use corn for biofuels. Thereupon the corn price rose that much that Mexicans could not afford tortillas any more. Tortillas are most consumed food in Mexico. This issue rose riots in the society.

R. T. Mathers, M. A. R. Meier, *Green polymerization methods*, Wiley-VCH, Verlag GmbH & Co. KGaA, Weinheim, Germany, **2011**.

V. Mittal, *Renewable Polymers*, Scrivener Publishing LLC, Salem, Massachusetts, **2012.**

P. Anastas, N. Eghbali, *Chem. Soc. Rev.*, **2010**, *39*, 301.

[1] United Nations Conference on Enviroment and Development (**1992**), Report of the United Nations Conference on Environment and Development, Rio de Janeiro. http://www.un.org/esa/sustdev. (accessed on 17. November 2014)

[2] G. Brundtland, *Our common future*, Oxfort University Press, Oxfort, **1987**.

[3] R. A. Sheldon, *Green Chem.* **2007**, *9*, 1273.

[4] K. van Aken, L. Strekowski, L. Patiny, *Beilstein Journal of Organic Chemistry* **2006**, *2*, 3.

[5] R. T. Mathers, M. A. R. Maier (Eds.), *Green Polymerization Methods*, Wiley-VCH, Verlag GmbH & Co. KGaA, Weinheim, Germany, **2011**.

3. Introduction to Polymer Synthesis

3.1 Step-Growth Polymerization

Step-growth reactions constitute one of the two polymerization reaction classes (chain-growth polymerization is the alternative reaction type). As implied by the name, these polymerization reactions proceed “step-by-step” and a large number of steps are required to form polymers of high molecular weight. In general, monomers of the type A-B or A-A and B-B, with A and B being functional groups, are suitable for step-growth polymerizations if the functional groups

can undergo formation of new bonds. Important examples are the formation of ester bonds from carboxylic acid and hydroxyl groups and the formation of urethane groups from the reaction between isocyanates and alcohols. If small molecules (X; e.g. H_2O, HCl, etc.) are eliminated in the course of the reaction the polymerization is named a polycondensation reaction (cf. **Figure 2**). If no molecule is eliminated it is named a polyaddition reaction.

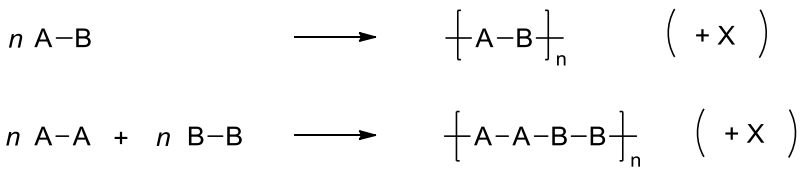

Figure 2: General reaction schemes for step growth polymerizations.

In the course of the step-growth reaction oligomeric (dimers, trimers, etc.) and polymeric intermediates are formed that feature the same functional groups as the underlying monomers in the absence of side reactions (cf. **Figure 3**). These intermediates possess more or less the same reactivity than the monomers and can undergo further reactions towards molecules with larger chain lengths.

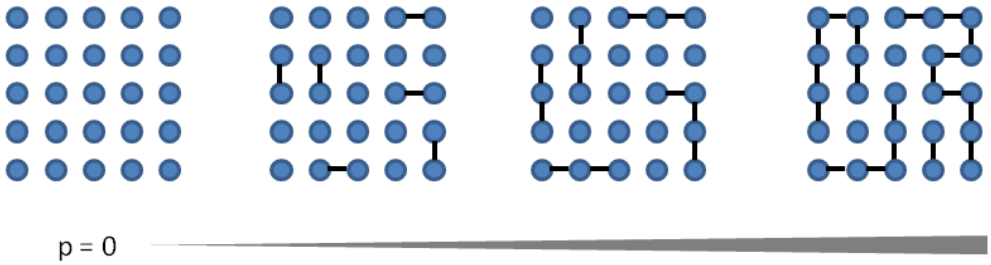

Figure 3: Progression of the step-growth reaction (blue spheres: monomer molecules; black lines: formed bonds between monomers).

It is easily discernible that in order to obtain polymers with high degrees of polymerization conversion has to be very high. A way to quantify the relationship between the extent of reaction and the degree of polymerization is given by the Carothers equation.

For step-growth reactions the number-average degree of polymerization $\bar{X}_n$ is defined as

$$\bar{X}_n = \frac{number\ of\ initially\ present\ molecules}{number\ of\ momentarily\ present\ molecules} = \frac{N_0}{N_t} \qquad (1)$$

For bifunctional monomers A-B and if the initial concentrations of the monomers A-A and B-B are identical, the degree of polymerization can be expressed as a function of the extent of reaction *p*:

$$\bar{X}_n = \frac{1}{1-p} \tag{2}$$

The plot of $\bar{X}_n$ versus *p* (**Figure 4**) illustrates the need for a very high conversion in order to achieve high degrees of polymerization and thus high molecular weights.

Once more it should be mentioned that equimolar amounts of monomers A-A and B-B are crucial for achieving conversions and high molecular weights (for monomers of the A-B type this is naturally no issue). In the case of different initial concentrations $[A\text{-}A]_0$ and $[B\text{-}B]_0$ the ratio *r* of these concentrations (or numbers of molecules) has to be taken into account and the Carothers equation changes to

$$\bar{X}_n = \frac{1+r}{1+r-2pr} \tag{3}$$

with

$$r = \frac{initial\ number\ of\ A-A\ molecules}{initial\ number\ of\ A-A\ molecules} = \frac{[A-A]_0}{[B-B]_0} < 1 \tag{4}$$

On the other hand it is easily possible to control the degree of polymerization by employing off-stoichiometric amounts of monomers since control via conversion is impracticable. Alternatively, off-stoichiometry can be achieved by using mono-functional endcapping agents, which have the additional advantage that the resulting polymer chain does not exhibit reactive ends that potentially undergo further reactions or degradation.

If the applied monomers feature more than two functional groups (e.g. triols such as glycerin), branched polymers and, eventually, polymer networks are formed. This process is accompanied by a drastic increase of the viscosity (at the gel point) and results in gelling of the reaction mixture. Prediction of the gel point is important in technical syntheses and can either be carried out by modifying the Carothers equation or using statistics (Flory and Stockmayer). In order to modify the Carothers equation the average functionality f_{av} of the monomers has to be determined.

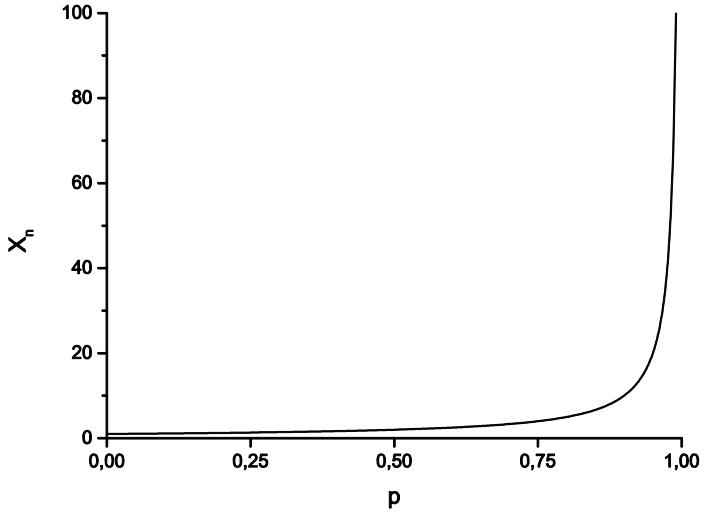

Figure 4: Relationship between $\bar{X}_n$ and p.

If N_j is the molecular quantity of monomer j and f_j its functionality (number of functional groups) f_{av} is defined as

$$f_{av} = \frac{\sum_j N_j f_j}{\sum_j N_j} \tag{5}$$

Utilizing the conversion p (and only in the case of a stoichiometric ratio of functional groups) one can therefore write for the degree of polymerization

$$\bar{X}_n = \frac{2}{2 - p f_{av}} \tag{6}$$

At the gel point $\bar{X}_n$ approaches infinity. As a consequence, conversion at the gel point p_{gel} is

$$p_{gel} = \frac{2}{f_{av}} \tag{7}$$

Further Readings

P. C. Hiemenz, T. P. Lodge, *Polymer Chemistry*, 2nd ed., CRC Press, **2007**.

B. Tieke, *Makromolekulare Chemie - Eine Einführung*, 2. Aufl., Wiley VCH, **2005**.

J. M. G. Cowie, *Polymers: Chemistry and Physics of Modern Materials*, 2nd ed., Blackie Academic & Professional, **1991**.

3.2 Chain-Growth Polymerization

Typically chain-growth is an addition polymerization reaction where unsaturated or cyclic monomers add onto the active sites of an initiator molecule or a growing polymer chain one at a time resulting in the growth of a chain on the active ends by addition of each monomer. Each monomer addition regenerates a new active site for the next addition. Depending on the initiator molecule such as mono-functional, di-functional and tri-functional species depicted in **Figure 5**, different polymer architectures can be achieved.

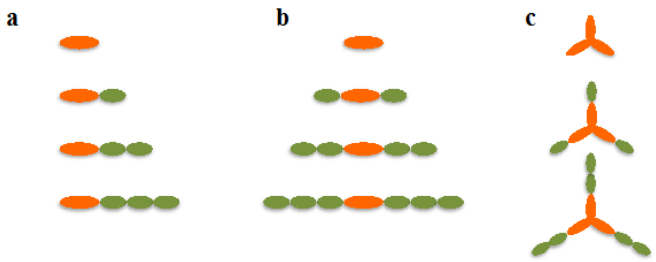

Figure 5: Schematic representation of different initiators for chain growth polymerization. Mono- (a), di- (b) and trifunctional (c) initiators and corresponding polymers.

In contrast to step-growth reactions, in chain-growth polymerization monomers add to the growing polymer chain much more rapidly with conversion (**Equation 8**). Alkenes, carbonyls and heterocycles can be polymerized by chain-growth mechanism.

$$(\text{-}M\text{-})_n + M \rightarrow (\text{-}M\text{-})_{n+1} \qquad (8)$$

Chain-growth polymerizations usually follow four steps:

1. Chain initiation by a compound with labile functional groups to generate a reactive intermediate. Typical active initiators and intermediates are: Free radicals, carbocations, carbanions and organometallic complexes in coordination/insertion polymerization. Carbonyls and heterocycles are not polymerized by radicals.

2. Chain propagation in which the active chain grows by each addition of monomer to the reactive chain end.

3. Chain transfer, which ceases the polymerization of an active chain and transfers the active site from one chain to another chain or monomer through a solvent, a transfer agent, a monomer or another polymer. This step can also lead to polymer branching.

4. Chain termination is a reaction that terminates the chain growth and the formation of reactive intermediates. Termination occurs either by recombination or disproportionation (cf. **Figure 6**).

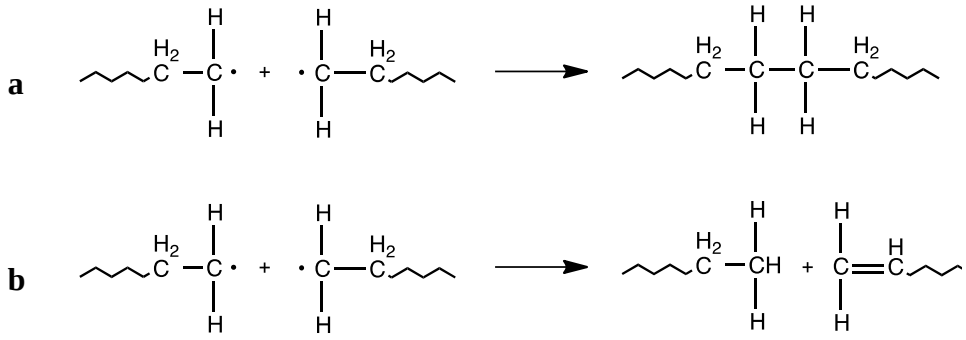

Figure 6: Termination reactions of active radical ends. (a) Recombination. (b) Disproportionation.

Chain-growth polymerization can be used to produce homo-polymers (**Figure 7, a**) consisting of one type of monomer repeating units or copolymers consisting of two or more types of monomers resulting in alternating (Figure 7, b), statistical or block copolymers (Figure 7, c). For more details, see copolymerization section (Chapter 3.4).

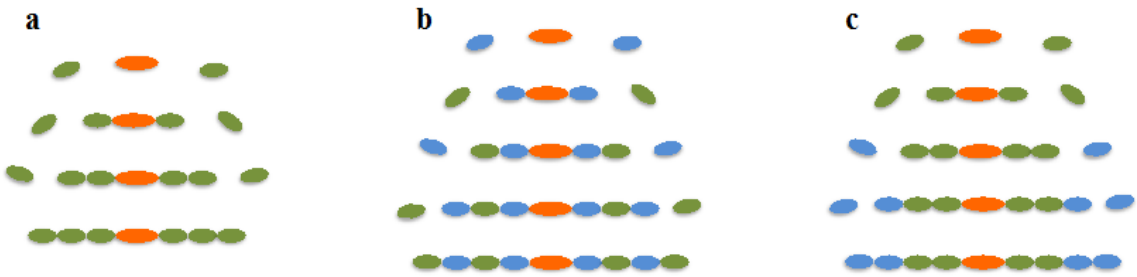

Figure 7: Schematic representation of different monomers for chain growth polymerization (a) Homo-polymer. (b) Alternating copolymer. (c) Block copolymer.

3.3 **R**ing **O**pening **P**olymerization (**ROP**)

Ring opening polymerization is a type of chain-growth polymerization initiated by reactive molecules that can open cyclic monomers. In the propagation step the reactive chain ends open cyclic monomers leading to polymer chain growth. Reactive initiators and propagating chain ends can be radical, anionic or cationic in nature. In ROP bond-angle strain relief and steric repulsions of ring atoms especially in heterocycles are the driving forces of ring opening reaction. Propagation can occur on different sites depending on the initiator active ends (cf. **Figure 8**).

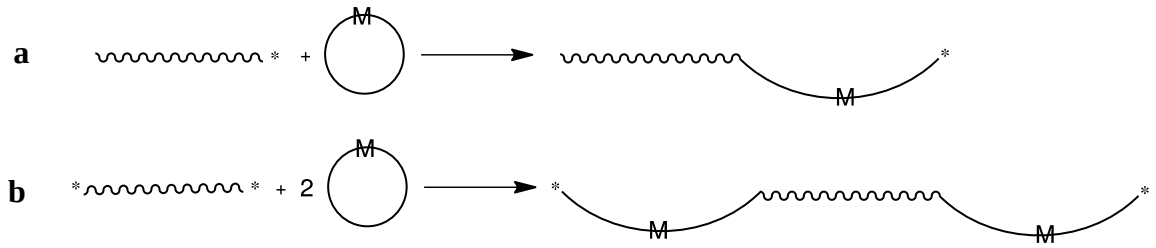

Figure 8: (a) Ring opening on one side of the initiator molecule or propagating chain. (b) Ring opening on both sides of the initiator molecule or propagating chain resulting chain growth on both sides.

ROP can polymerize cyclic monomers containing heteroatoms or without heteroatoms in the ring structure. The following structural units are often observed in monomers for ROP:

1. Compounds containing the following heteroatoms in the ring and corresponding monomers:
    a. oxygen: ethers, acetals, esters (lactones, lactides, and carbonates), anhydrides
    b. sulfur: polysulfur, sulfides and polysulfides
    c. nitrogen: amines, amides, lactames, imides, N-carboxyanhydrides and 1,3-oxaza derivatives
    d. phosphorus: phosphates, phosphonates, phosphites, phosphines and phosphazenes
    e. silicon: siloxanes, silathers, carbosilanes and silanes
2. Compounds containing no heteroatoms in the ring:
    a. alkanes
    b. alkenes

Ring opening polymerization plays a major role in the synthesis of biomaterials with high molecular weight and low dispersity.

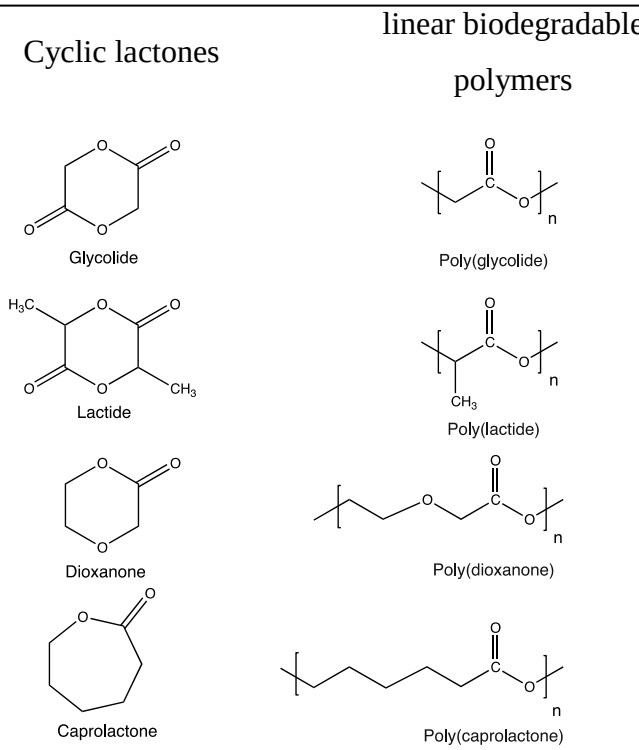

Figure 9: Lactones and their corresponding biodegradable polymers.

Biodegradable biopolymers such as polylactones or polyesters, which can undergo hydrolytic degradation of the ester bonds, can be produced by ROP or polycondensation. For biomedical purposes, ROP is favored over polycondensation, as there is no need to azeotropically remove water from the reaction to form the polymer. Furthermore, ROP offers better control on molecular weight and dispersity while requiring milder reaction conditions. Cyclic lactones can yield biodegradable linear polymers by ROP (cf. **Figure 9**).

The mechanism of ring opening polymerization can follow different pathways depending on the initiator. Here, we introduce three mechanisms by exemplifying common examples. Polydimethylsiloxane (PDMS) is a subgroup of organosiloxanes, better known as silicones. Since their first introduction in the 1940s, they have been categorized as an important class of polymers with special properties such as uncommon rheological behavior (flow), inert inorganic backbones, optical transparency and very good thermal stability. Additional properties such as physiological inertness, high blood compatibility, low toxicity, oxidative stability, low modulus and anti-adhesive properties have made PDMS the polymer of choice for many biomedical applications. Polymerization of PDMS with high molecular weights is based on ROP. Ring opening of cyclic siloxanes (**sil**icon, **ox**ygen and alk**ane** compounds) with three or four siloxane groups can undergo an anionic (**Figure 10, a**) or a cationic (Figure 10, b) mechanism. Depending on the degree of polymerization, a range of PDMS polymers

from low molecular weight (liquid, also referred to as silicone oil) to high molecular weight (solid elastomer) with different mechanical properties can be achieved.

Since the introduction of polylactic acid (PLA) as a material for resorbable sutures, implants, and drug-delivery systems in 1954 by DuPont de Nemours and Ethicon, Inc., the use of PLA as a biodegradable and biocompatible material has steadily increased. This can be explained with its degradation to lactic acid, a natural occurring non-toxic chemical that can be metabolized in the tricarboxylic acid cycle and excreted from the body.

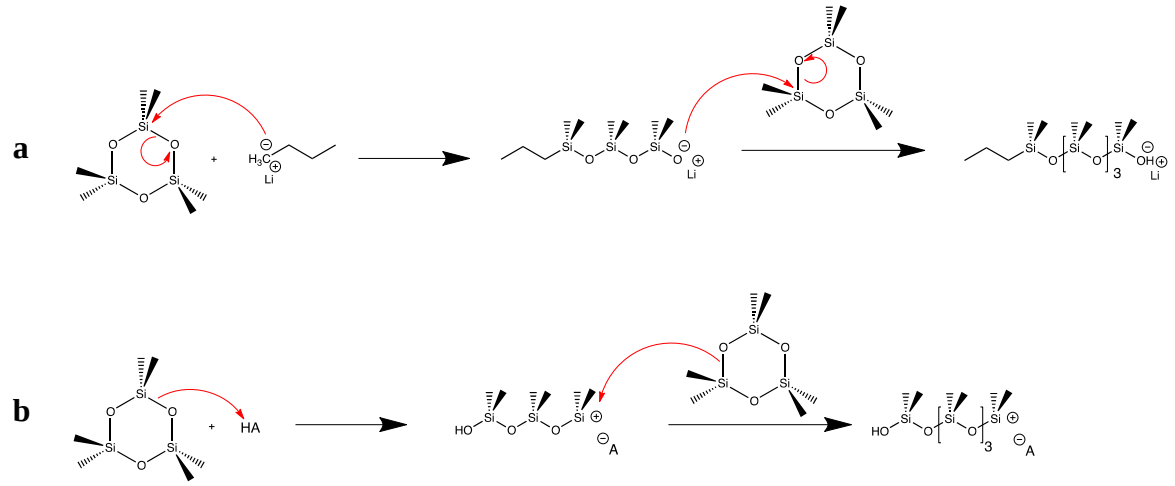

Figure 10: Mechanism of ring opening polymerization of D_3 from (a) Anionic pathway initiated by BuLi and (b) Cationic pathway initiated by an acid to yield PDMS.

Besides polycondensation of lactic acid, ROP of cyclic lactone (lactic acid dimer) is an optimal synthesis pathway to obtain high molecular weight PLA. In order to initiate the ROP reaction and to polymerize the lactide monomer with retention of configuration, a range of metal alkoxide initiators has been reported. Among all these organometallic catalysts, tin(II) 2-ethylhexanoate found a special place in biomaterials synthesis due to its solubility in many lactones and organic solvents, its low toxicity, FDA (U.S. **F**ood and **D**rug **A**dministration) approval, high catalytic activity and its ability to give high molecular weight polymers with low racemization. For the ROP of the cyclic lactide monomer, two major ring-opening mechanisms have been proposed:

(a) Activated monomer mechanism

(b) Coordination-insertion mechanism

Both mechanisms are alcohol-initiated since the degree of polymerization is clearly dependent on the monomer to alcohol ratio, and because the end groups of the corresponding polymer

carry hydroxyl functions. The proposed coordination-insertion mechanism for ROP of lactide initiated by $Sn(Oct)_2$ involves four steps (cf. **Figure 11**):

1. Coordination of the lactide monomer to the Lewis-acidic metal center.
2. Insertion of lactide monomer into the metal-alkoxide bond via nucleophilic addition.
3. Ring opening of the lactide monomer *via* acyl-oxygen cleavage and continuous insertion of lactide monomers.
4. Termination of the polymerization reaction by hydrolysis of the active propagation chain, which is performed before isolation of the PLA.

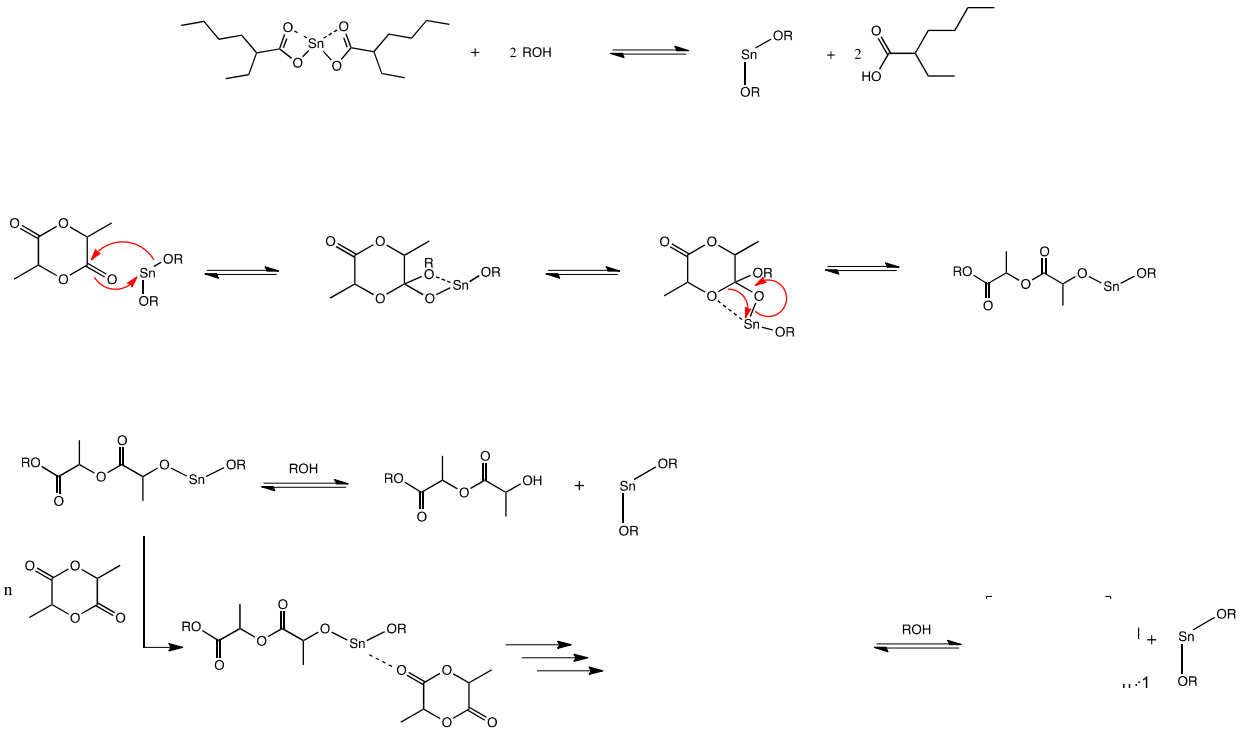

Figure 11: Proposed coordination-insertion mechanism for ROP of lactide initiated by a hydroxyl-functionalized molecule and $Sn(Oct)_2$.

3.4 Copolymerization

Copolymerizations are polymer reactions in which different monomers are linked together to form a copolymer. Many important materials of daily life are in fact copolymers which highlights the great importance of the copolymerization process. This derives from the fact that many of the desired material properties can be generated by combining properties of different monomers in copolymers rather than by blending the respective homopolymers. Prominent examples are acrylonitrile butadiene styrene (ABS) and styrene acrylonitrile resin

(SAN) that exhibit properties superior to "pure" polystyrene especially in terms of mechanical strength. Moreover, many biopolymers such as proteins can be considered as copolymers.

Copolymers can be classified into different types according to the structural make-up of the architecture (cf. **Figure 12**). Whereas random copolymers (a) and alternating copolymers (b) are mostly synthesized via radical polymerization methods, block copolymers (c) and graft copolymers (d) are furthermore accessible by controlled radical polymerization, ionic polymerization and step-growth reactions.

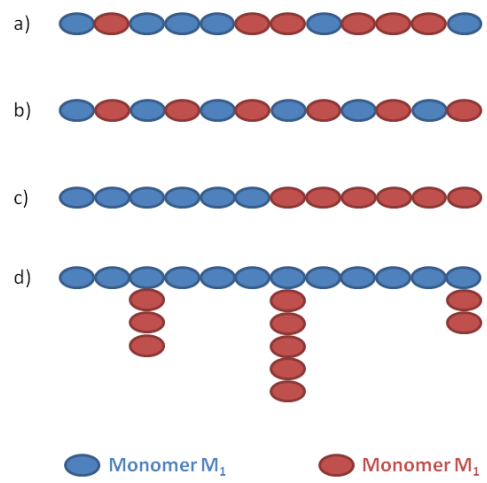

Figure 12: Schematic representation of copolymer structures: a) random copolymer; b) alternating copolymer; c) block copolymer; d) graft copolymer.

The composition of a copolymer as a crucial material parameter can be determined as a function of the monomer feed ratio. Of importance are mainly the rate constants of the chain growth reactions and the ratios thereof. For that reason, we take a look at the radical polymerization of two monomers (M_1 and M_2). Since now there are two different active chain ends (compared to one in the homopolymerization of M_1 or M_2), four chain growth reactions are conceivable (initiating and termination reactions are ignored):

$$-M_1^* + M_1 \xrightarrow{k_{11}} -M_1M_1^* \quad (9)$$

$$-M_1^* + M_2 \xrightarrow{k_{12}} -M_1M_2^* \quad (10)$$

$$-M_2^* + M_1 \xrightarrow{k_{21}} -M_2M_1^* \quad (11)$$

$$-M_2^* + M_2 \xrightarrow{k_{22}} -M_2M_2^* \quad (12)$$

The corresponding reaction rates are

$$v_{11} = k_{11}[-M_1^*][M_1] \tag{13}$$

$$v_{12} = k_{12}[-M_1^*][M_2] \tag{14}$$

$$v_{21} = k_{21}[-M_2^*][M_1] \tag{15}$$

$$v_{22} = k_{22}[-M_2^*][M_2] \tag{16}$$

The ratio of the rates of consumption of the two monomers equals the average ratio of the two monomer species in the copolymer (the "concentration" of the monomers in the copolymer chain) and can be written using the rates of the monomer depletion reactions:

$$\frac{-d[M_1]/dt}{-d[M_2]/dt} = \frac{v_{11} + v_{21}}{v_{22} + v_{12}} \tag{17}$$

If we substitute equations (13) to (16) and consider the concentration of the active chain ends (radicals) as steady (Bodenstein's law)

$$v_{21} - v_{12} = v_{12} - v_{21} = 0 \tag{18}$$

we obtain the Mayo-Lewis equation:

$$\frac{d[M_1]}{d[M_2]} = \frac{[M_1]}{[M_2]} \frac{\frac{k_{11}}{k_{12}}[M_1] + [M_2]}{\frac{k_{22}}{k_{21}}[M_2] + [M_1]} \tag{19}$$

The Mayo-Lewis equation allows the determination of the copolymer composition at any given moment during the copolymerization as a function of the momentary ratios of the monomer concentrations. However, this composition is not necessarily the final composition of the copolymer since the monomer ratio is subject to change in the course of the reaction. The reactivity ratios r_1 and r_2 are defined as the ratios of the respective rate constants of the chain growth reactions:

$$r_1 = \frac{k_{11}}{k_{12}} \tag{20}$$

$$r_2 = \frac{k_{22}}{k_{21}} \tag{21}$$

These ratios can be experimentally determined and are useful to estimate the copolymer composition that can be expected for a given pair of monomers. The following combinations are conceivable:

- $r_1 \cdot r_2 = 1$: random copolymerization (if $r_1 = r_2 = 1$: ideal copolymerization)
- $r_1 \cdot r_2 < 1$: alternating copolymerization (if $r_1 = r_2 = 0$: perfectly alternating)
- $r_1 >> 1$, $r_2 >> 1$: block copolymer (extreme case: formation of homopolymer)

A convenient way to illustrate the composition of the copolymer as a function of the monomer ratio is the so called copolymerization diagram. The mole fraction F_1 of monomer M_1 in the copolymer is plotted against the mole fraction f_1 of monomer M_1 in the reaction feed. **Figure 13** gives examples for different copolymerization systems.

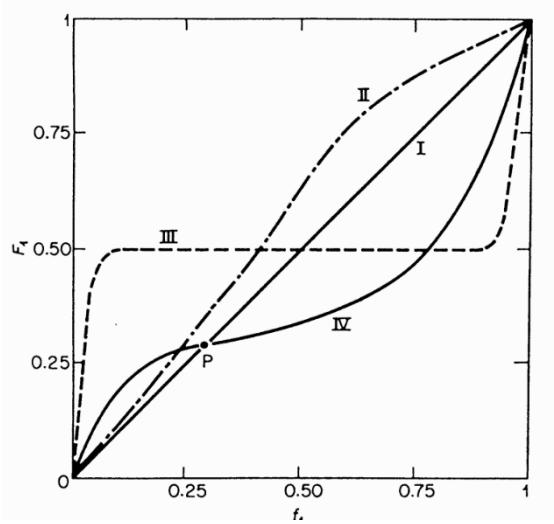

Figure 13: Copolymerization diagram for I) ideal copolymerization; II) random copolymerization with slight preference for the incorporation of monomer M1; III) (perfectly) alternating copolymerization; IV) border case between random and alternating copolymerization.

Further Readings

P. C. Hiemenz, T. P. Lodge, *Polymer Cemistry*, 2nd ed., CRC Press, **2007**.

B. Tieke, *Makromolekulare Chemie - Eine Einführung*, 2. Aufl., Wiley VCH, **2005**.

J.M.G. Cowie, *Polymers: Chemistry and Physics of Modern Materials*, 2nd ed., Blackie Academic & Professional, **1991**.

4. Introduction to NMR spectroscopy

NMR (nuclear magnetic resonance) spectroscopy is one of the main analytical methods in the field of polymer chemistry: The key facts are:

- Applicable over a wide temperature range (approximately -190 to +300°C)
- Not destroying the material under investigation
- Provides a plenty of chemically and physically relevant information
- Used not only in research but also in industry (e.g. production control) or in medicine

In macromolecular chemistry molecules are usually studied in solution. The main applications of NMR-spectroscopy in polymer science are:

- Identification of the molecule and its constitution
- Kinetics and mechanism of polymerization
- Determination of tacticity in stereospecific macromolecules
- Sequence analysis in the case of copolymers and cis-trans-isomerism
- Determination of end groups, short-chain branches, and other defects

4.1 Fundamentals of NMR spectroscopy

Prerequisite for nuclear magnetic resonance spectroscopy is the presence of nuclei having a nuclear spin unequal to zero. The principle of NMR spectroscopy is based on the interaction of the magnetic moment of the nuclear spin with an external magnetic field. In the absence of an external magnetic field, the magnetic moments of individual nuclei do not exhibit a preferred direction. However, in a homogeneous static magnetic field B_0 they are oriented, i.e. the degeneracy of the possible states will be canceled and there is a split leading to the so-called Zeeman states. The nuclear spin can only adopt 2I + 1 (I: spin quantum number) orientations. For a nucleus with the spin quantum number I = 1/2 (e. g. ^{1}H, ^{13}C), there are thus only two possible orientations in the magnetic field, and thus two different energy levels. The energy difference ΔE between these two nuclear Zeeman levels depends on the strength of the magnetic field B_0 as follows:

$$\Delta E = \gamma \hbar B_0 \quad (22)$$

γ: Gyromagnetic ratio

$\hbar$: Reduced Planck's constant = $h/2\pi$

This energy difference ΔE leads to a difference in the population of the energy states. The sum of the z-components of all magnetic moments results in a macroscopic magnetization M_0 in the direction of the magnetic field. According to the resonance condition transitions between energy levels by irradiating an additional field B_1 at the proper frequency ν_1 (Larmor frequency) can be induced.

$$\Delta E = \hbar \nu_l \quad (23)$$

To satisfy the resonance condition, the frequency ν_0 can be either varied at constant field strength (frequency sweep) or the field B_0 is varied at constant frequency ν (field-sweep). In both methods, the individual resonances are successively detected by continuous change of ν_0 or B_0. This is referred to a so-called CW (continuous wave) mode. In modern pulsed FT-NMR spectrometers, however, all cores are excited simultaneously by a high-frequency generator. The receiver of the spectrometer detects the decay of the transverse magnetization generated by the pulse. The decay of transverse magnetization is called free induction decay (FID). This signal is a complex interferogram of superimposed damped oscillations. By applying Fourier transformation the time-dependent signal is converted into the frequency spectrum (cf. **Figure 14**).

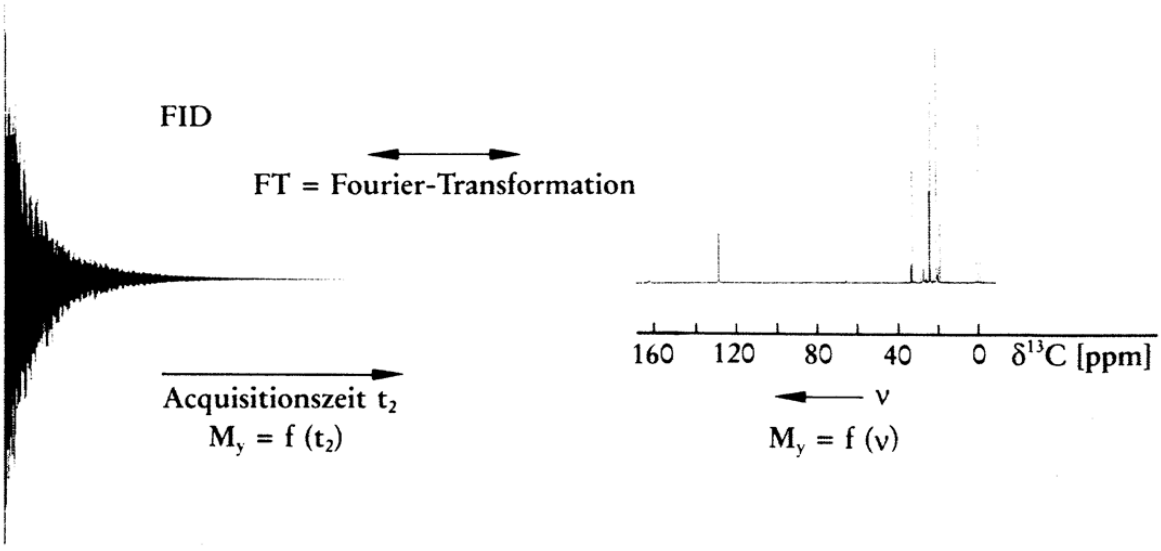

Figure 14: Fourier transformation: Conversion of the time signal into the frequency spectrum.

4.2 Chemical shifts

In diamagnetic molecules the magnetic field at the nucleus B_{eff} is always smaller than the applied field. The cores are shielded by the electrons and the other atoms around.

$$B_{eff} = B_0 (1 - \sigma) \tag{24}$$

σ = shielding constant

Within a molecule, the electronic neighborhood of different protons (or ^{13}C atoms, etc.) is usually different so that different resonance frequencies occur, and thus the signals appear at various positions in the spectrum. In practice, the frequencies are measured relative to a standard. In order to eliminate the field dependence of the measuring effect, one introduces the so-called chemical shift:

$$\delta\,[\text{ppm}] = \frac{\nu_{sample} - \nu_{standard}}{\nu_{standard}} \times 10^6 \tag{25}$$

NMR shifts of common laboratory solvents are listed in the publication from Gottlieb *et al*.[1]

Caused by bonding electrons, an indirect spin-spin coupling occurs between adjacent cores (scalar coupling, J-coupling). This occurs as a fine structure of the signals in the spectrum and provides important information about the structure of the molecule. The size of the coupling constant is independent of the magnetic field strength and is up to 15 Hz for protons. It contains information about the type and the number of bonds between the coupled nuclei. The signals in the spectra can be integrated to receive the number of protons which generate the signal. Chemical shifts, coupling constants, fine structure of the signals and the intensity ratios are used to identify the compound by information provided by the NMR spectrum.

Integration of the signals in the ^1H-NMR spectrum leads to the ratios between the signals and so the quantity of protons can be determined. In contrast to the ^1H-NMR spectra, the signals of ^{13}C-NMR spectra usually can´t directly be integrated to obtain quantitative information about the number of carbon atoms. In order to increase the readability of ^{13}C-NMR spectra, the routine ^{13}C-NMR spectrum is broadband proton decoupled. This technique suppresses the coupling between carbon and hydrogen nuclei and for different carbon nuclei only individual signals are obtained instead of multiplets. On one hand this results in a considerable increase

in signal intensity (nuclear Overhauser effect) and in a simplification of the spectra, but on the other hand the spectra usually cannot be evaluated quantitatively.

Nevertheless, one possibility to obtain quantitative information is provided by the so-called inverse gated decoupling, a special measuring method, wherein the decoupler is switched on only during the ^{13}C measurement pulses and during the FID, but not in the subsequent dwell time. Spin-lattice relaxation and nuclear Overhauser effect do not influence signal intensity then, and the spectrum can be evaluated quantitatively. The disadvantage of this method is the relatively long measurement time.

4.3 Two-dimensional NMR spectroscopy DOSY (diffusion ordered spectroscopy)

Using pulsed gradients, the diffusion coefficient of soluble polymers may be determined by NMR spectroscopy. This measurement technique is based on performing a spatial encoding of the spin positions and to determine this parameter at two different times. So the distance between the two positions can be detected. The diffusion coefficient D depends on,

$$D = \frac{kT}{6\pi\eta_s R_H} \tag{26}$$

where η_s is the viscosity of the solvent, R_H the hydrodynamic radius, k is the Boltzmann constant and T is the absolute temperature. The hydrodynamic radius is directly proportional to the radius of gyration R_g. The proportionality depends on the coiled shape of the polymer chain. The main use of this NMR technique in polymer science the identification of low molecular weight compounds (monomers, solvents, etc.) in a high molecular weight sample.

Further Readings

H.-G. Elias, *Makromoleküle*, Hüthig & Wepf Verlag, Basel Heidelberg, **1971**, S 87 ff.

M. D. Lechner *et al*., *Makromolekulare Chemie*, Birkhäuser Verlag, Berlin, **1993**.

H. Günther, *NMR-Spektroskopie*, 3.Auflage, Georg Thieme Verlag, Stuttgart, **1992**.

H. Friebolin, *Ein- und zweidimensionale NMR-Spektroskopie*, VCH Weinheim, **2013**.

M. Hesse, H. Meier, B. Zeeh, *Spektroskopische Methoden in der organischen Chemie*, Georg Thieme Verlag, Stuttgart, **2011**.

[1] H. E. Gottlieb, V. Kotlyar, A. Nudelman, *J. Org. Chem.* **1997**, *62*, 7512.

5. Introduction to Size-Exclusion Chromatography (SEC)

In contrast to low molecular weight organic compounds which have discrete molecular weights, synthetic polymers usually consist of a variety of chains of different length. This molecular weight distribution affects all essential properties of the corresponding polymer. Therefore, a core component of polymer analysis is the determination of molecular weight distributions. Size-exclusion chromatography (SEC) is the most commonly used method for the determination of molecular weight distributions in the polymer sector. The main principle of a SEC setup is based on pumping a dilute solution of the polymer of consideration through a column which is filled with a porous gel. The column is directly connected to at least one detector which measures the concentration of polymer as a function of elution volume (elugram).

The separation of polymers within the SEC columns is based on interactions of the dissolved chains with the pores of the gel material. The dimensions of the gel pores need to be on the same order of magnitude as the hydrodynamic radius of the chains to be examined. Chains which are too large to penetrate into the pores pass through the column without retardation. The volume of solvent which is needed to transport these chains through the column is called upper exclusion volume V_0. It is equal to the difference between the total column volume and the volume occupied by the gel structure, as well as the inner gel volume V_i. A macromolecule, however, which is so small that it can penetrate into all pores, leaves the column to the lower exclusion elution volume V_u. Macromolecules that can, due to their size, only penetrate a section of the pores are eluted with an elution volume V_{el} which lies between the two cutoffs V_u and V_0. This elution volume is dependent on the hydrodynamic volume and thus also on the molecular weight of the polymer. The smaller the polymer, the longer it remains in the column and the greater is the elution volume. The exact relation between molecular weight and elution time must be determined experimentally (calibration) in each case for the existing system as it is not accessible from theory. This function depends on factors such as the solvent, combination of columns, gel material, temperature, back pressure or flow rate of the column. If the function is known, the molecular weight distribution can be calculated from a measured elugram.[1,2]

5.1 Determination of the molecular weight distribution

The standard method for the analysis of SEC elugrams consists in the application of a calibration relationship for the calculation of the molecular weight distribution. The calibration relationship between molecular weight and elution volume is determined experimentally. Standard polymers with very narrow molecular weight distributions and known molecular weight can be used to calibrate the SEC system. The calibration relationship is then determined from a plot from the respective molecular weight vs. elution volume. This function can be used to calculate the molecular weight distribution from the elugrams of the polymers of consideration. However, this approach is only completely correct when the measured polymer possesses the same constitution and is composed of the same monomer repeat units as the standard polymer used. In addition, the solvent quality relating to the polymer to be measured should not deviate too much from the solvent quality relating to the calibration polymer system. The problem is that the separation depends on the hydrodynamic volume and not on the molecular weight of the sample. Thus, branched macromolecules with the same molecular weight generally have a much smaller hydrodynamic volume than linear polymers. Therefore, the use of linear polymers for calibration leads to underestimated molecular weights while determining the distribution of branched systems, and the error can exceed 100%. For a given molecular weight, a difference in solvent quality between the calibration system and the system to be measured leads to a deviation of the hydrodynamic volume. The problems described are often circumvented by means of a universal calibration curve. Here, it is assumed that the hydrodynamic radius is proportional to the product of the Staudinger index and molecular weight. This approach allows determining molecular weight distributions of branched polymers or other polymers for which calibration standards are not available with the help of linear calibration polymers. This will only work if the relationship between the intrinsic viscosity and the molecular weight of the branched system is known. This relationship is experimentally difficult or not accessible in branched systems, which greatly limits the use of a universal calibration curves. The advantage of using a calibration curve lies in the minimal effort of equipment.

Combining a fractionation method with a flow-light scattering detector an absolute determination of the molecular weight distribution of a sample can be achieved. A calibration with standard polymers is not required in this case. Meanwhile, a variety of different light scattering systems with flow cells are available. A frequently used system is the small-angle light scattering (SALS). In this method, the light is scattered at a fixed angle of 6-7° or 15°

(depending on the device). Other systems permit the measurement at a plurality of angles, such as the two-angle light scattering (TALS) or the multi-angle light scattering (MALS). In MALS the scattered light is measured in up to 18 different angles at each time. The theoretical fundamentals of SALS correspond to those of the static light scattering. Due to the small angle measurement, however, the particle scattering factor can be neglected. In an ideal case, only polymers with identical molecular weights are located in the detector cell at a defined point of time. In this case the measured molecular weight corresponds to the actual molecular weight of each macromolecule. In real systems different molecular weights are eluted at the same time. In branched polymers the problem occurs that less branched molecules have the same hydrodynamic volume as more highly branched molecules with higher molecular weight. At any time of the experiment a monodisperse polymer mixture cannot be found in the detector cell. Consequently, the measured molecular weight is similar to the static light scattering an average (weight average) of the eluated molecules. In the evaluation of SALS measurements, the molecular weight can be calculated directly from the reciprocal scattering intensity and concentration. Thus, the molecular weight distribution, the molecular weight averages and the polydispersity can be obtained.

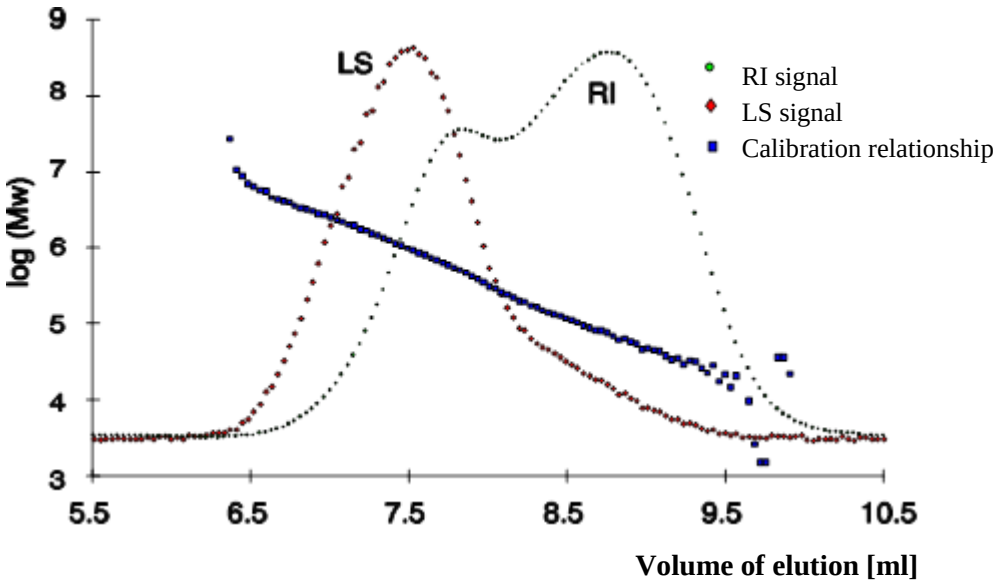

Figure 15: Overlay of LS and RI elugrams with the values derived from both elugrams to receive the calibration relationship.

In contrast to SALS the particle scattering factor is considered while performing MALS (or TALS) which allows the determination of the radius of gyration. In the light scattering flow cell angle-dependent elugrams are measured which are dependent on the square of the average

radius of gyration of the measured macromolecules. Thus, the size of the eluted particles can determined at any time.

By using a refractive index detector (RI) or a UV detector in case the chains are UV active, purely concentration-dependent elugrams can be recorded. Based on the measured elugrams from the light scattering detector and from the RI detector the molecular weight distribution and the distribution of the radii can be calculated. As a result, the number-average and weight-average molecular weight and radius of gyration as well as the dispersity are obtained. **Figure 15** shows an overlay of the detector signals and of the calibration curved received from both elugrams.

5.2 SEC setup

The setup of a SEC system with triple detection, i.e. small-angle light scattering with a combined refractive index/viscosity detector, is shown in **Figure 16**.

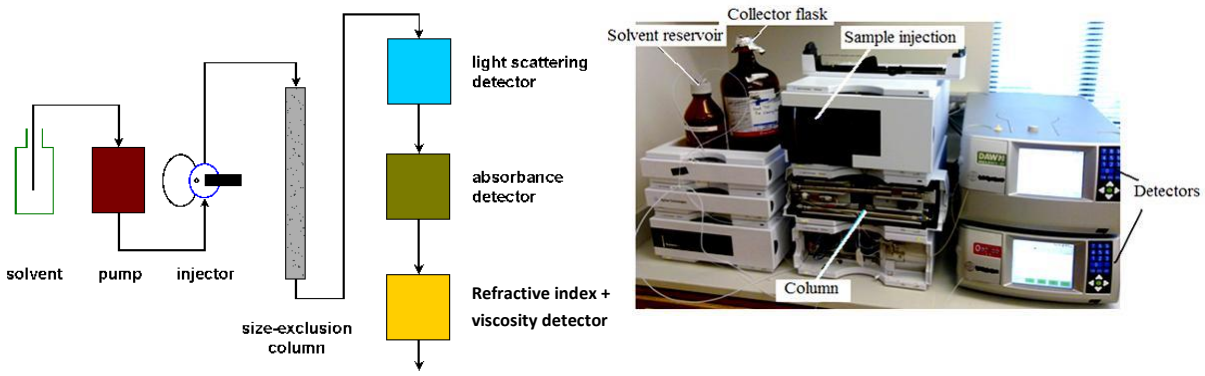

Figure 16: Schematic setup (left) and photograph (right) of a SEC equipment.
Triple-detection: SEC system with concentration detector (RI/UV), light scattering detector (MALS or LALS) and viscosity detector

The solvent is pumped from a solvent reservoir through the columns and detectors by a pump. A degasser is often used between the solvent reservoir and the pump to remove air from the solvent, which is important for obtaining a good baseline. An injector is located between pump and columns, through which the dissolved and filtered polymer solution is injected into the system. The column set usually consists of several columns with different pore sizes. A typical column combination is: pre-column (to remove dust), 10^5 nm column, 10^4 nm column, 10^3 nm column and finally a 10^2 nm column. Such a combination of columns is able to

separate polystyrene samples into molecular weight fractions of about 500 D to about 5000000 D. The combination of columns is often placed in a column oven to ensure a defined temperature. After the column set the detectors are installed with the RI detector usually being installed as the final detector.

Bibliography:

[1] W.W. Yau, J.J. Kirkland, D.D. Bly, *Modern Size Exclusion Liquid Chromatographie*, John Wiley, NewnYork, **1979**.

[2] S. Mori, H. G. Barth, *Size Exclusion Chromatography*, Springer Berlin, **1999**.

6. Introduction to MALDI-ToF-MS

Mass spectrometry is an analytical technique which determines molecular weights of free ions in a high vacuum with the aid of a mass spectrometer. A mass spectrometer typically consists of an ion source, in which the analyte is ionized, a mass analyzer, where the ions are separated according to their mass-to-charge ratio (m/z) and a detector which detects the number of the corresponding ions. **Figure 17** shows the setup of a mass spectrometer schematically.

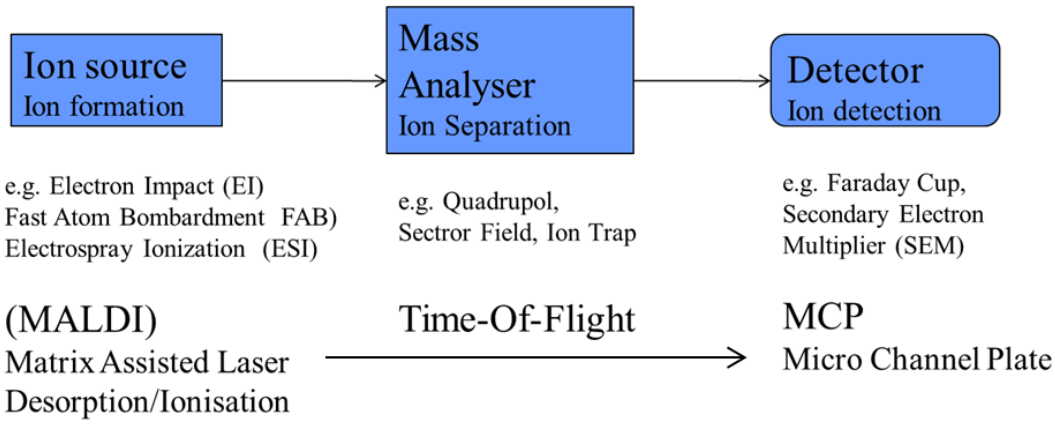

Figure 17: Setup of a mass spectrometer.

Ionization of the sample can be carried out by the addition or elimination of electrons. This process can take place by electron impact (EI), by bombardment with ions or atoms (fast bombardment ionization, FAB) or by photons (laser desorption/ionization, LDI). Injecting a sample in an electric field is a further possibility to ionize (electro spray ionization, ESI).

The separation of the ions can be based on different physical principles. In sector field instruments, the separation is achieved by deflection based on electric or magnetic fields. In alternating fields, ions of various masses can be filtered (quadrupole, ion trap). With flight analyzers (time-of-flight, TOF) the separation is based on the different flight time of the ions in the field-free space.

The matrix-assisted laser desorption ionization time-of-flight mass spectroscopy (MALDI-TOF-MS) is a rapid and sensitive method for the determination of absolute molar masses of large molecules. In special cases, molecular weights can be determined up to 200000 g mol^{-1}. Normally, molecular weights from 500 to 100000 g mol^{-1} are accessible. In the case of narrow molecular weight distributions (dispersity <1.2) the method allows the determination of the molecular weight distribution as well as the number average and weight average molecular weights. For broader molecular weight distributions only the low molecular weight portion of the distribution is usually seen.

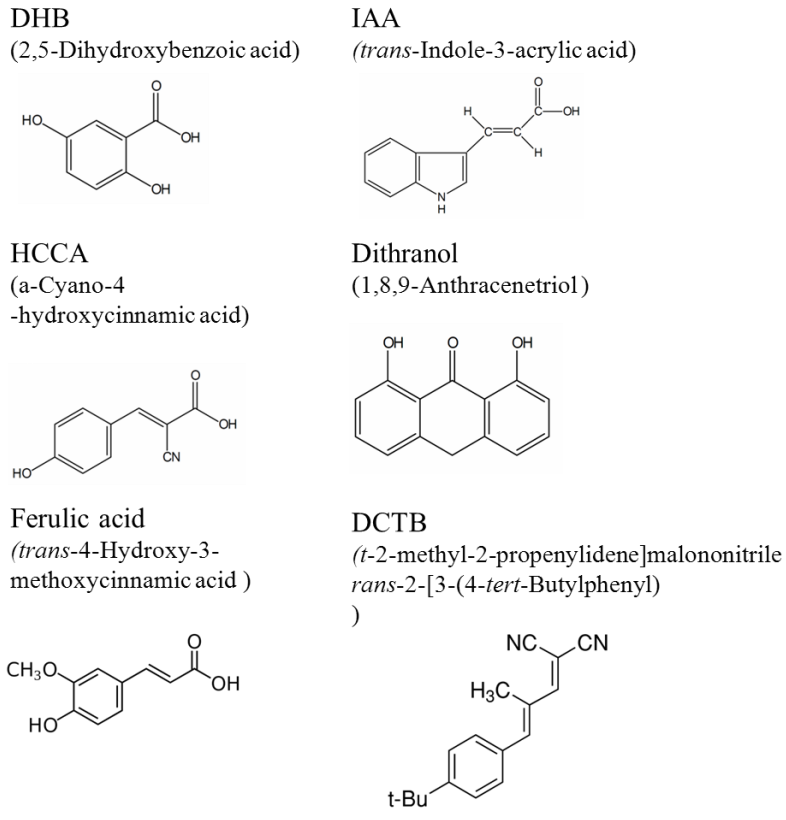

Figure 18: Some matrices used in MALDI-ToF MS.

In MALDI-ToF, polymer chains are diluted in a low molecular weight matrix, vaporized unscathed and ionized by laser bombardment. Therefore, the sample to be measured is mixed with a concentrated solution of the matrix. Typical matrices used in MALDI-ToF MS are shown in **Figure 18**. Suitable matrix molecules are mainly higher conjugated aromatic

compounds, which are readily miscible with the polymer samples, do not react with the polymer and possess an absorption maximum in the UV range of the incident laser light. The choice of a certain matrix for a particular measurement depends on the polarity of the polymer sample. Hydrophilic polymers require hydrophilic matrices, while hydrophobic polymers are measured with hydrophobic matrices. The matrix is often in a 1000 to 10000 times excess. For improving ionization, a salt is added to the mixture. The choice depends on the polarity of the polymer, too. In most cases, silver or alkali metal salts (e.g. NaCl, NaTFA, AgTFA, LiBr) can be used. The mixture is then dropped onto a target and after evaporation of the solvent a semi-crystalline layer results in which the polymer molecules are completely separated from each other by matrix molecules.

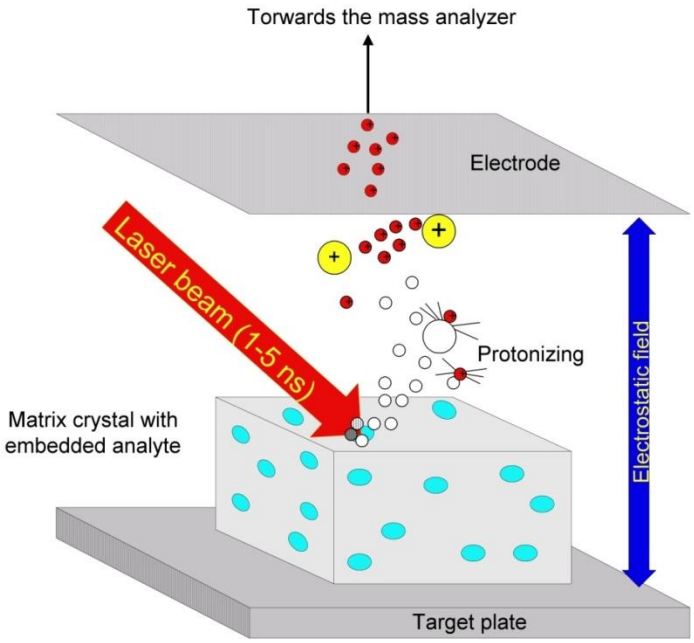

Figure 19: Principle of ionization in the ion source of a MALDI-MS.

The ions are generated in high vacuum by a high energy laser pulse targeting the matrix-embedded sample (cf. **Figure 19**). As a result of the laser bombardment, ionization occurs through the resonant excitation of the matrix molecules. There is a phase transition in which a portion of the solid sample surface evaporates explosively. In this step, the matrix molecules and hence the embedded polymer molecules are transferred into the gas phase. The photo-ionized radical in the matrix molecules are transferred on the polymers and thus ionized, non-fragmented polymer ions are produced in high yield. This is an important difference compared to conventional mass spectrometry, during which analyte fragmentation frequently occurs. An electrostatic field is applied which accelerates the ions towards the analyzer. After leaving the ion source, the ions enter a time-of-flight analyzer, in which separation according to their mass to charge ratio (m/z) takes place. For a given kinetic energy, chains with different m/z ratio are accelerated to different speeds. For this reason, heavier molecules reach the detector later than lighter molecules with same charge. If the acceleration voltage U and the length in field-free space are known, the flight time of different m/z ratios can be determined according the following equation.

$$t_{total} = const \times \sqrt{\frac{m/z}{U}} \tag{27}$$

During the ionization process not all ions are generated exactly at the same time and in the same place. This leads to an inaccuracy in space and time, and thus to an energy distribution of the ions formed. As a result, not all ions with the same m/z ratio exhibit the same energy. Thus, these molecules don´t exactly impinge on the detector at the same time, resulting in decreased resolution of the detector. This principle is shown in **Figure 20**. One way to circumvent peak expansion and to increase resolution is the use of a reflector system.

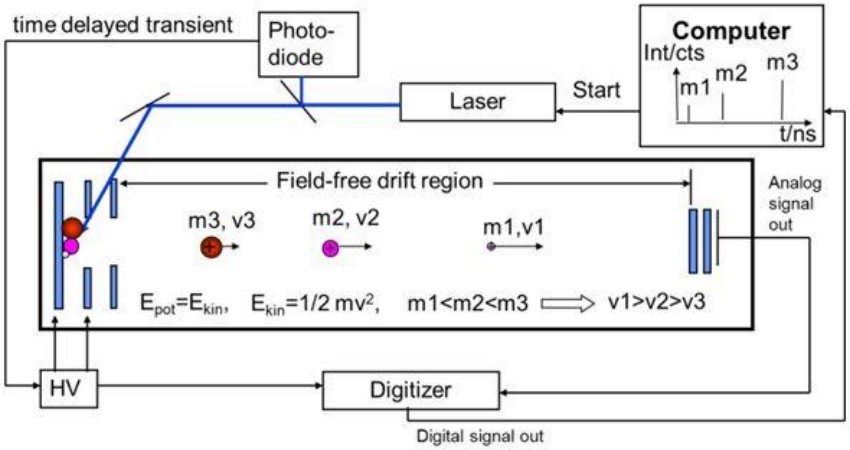

Figure 20: Principle of a linear MALDI-TOF-MS.

The operation is based on an inversion of the ion cloud in an oppositely polarized electromagnetic field. This field is directly attached to the end of the field-free flight region. Ions with the same m/z ratio, but slightly higher kinetic energy are able to penetrate deeper into the field than ions with lower kinetic energy. Thus, ions with a higher energy have to travel a larger distance. By suitable choice of field strength, ions with the same m/z ratio but with different speed can be focused, which results in a massive improvement in the detector resolution. The principle of a reflector MALDI-TOF-MS is illustrated in **Figure 21**. Depending on the polarity of the applied field, both negatively charged and positively charged ions can be analyzed.

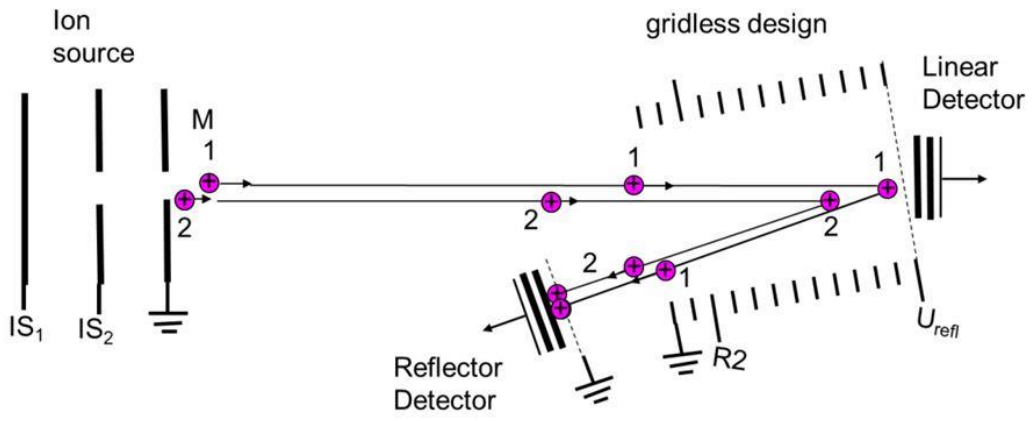

Figure 21: Illustration of a reflector used in MALDI-TOF-MS.

In MALDI-TOF-MS, data are usually displayed as number-fraction intensity vs a linear mass scale. In SEC however, the weight-fraction intensity is displayed vs a log mass scale. In order to compare data of SEC and MALDI-TOF-MS it is necessary to convert them into the same type of distribution. Furthermore, in contrast to SEC, discrete molecular weight distributions are obtained by MALDI-TOF-MS. Each signal corresponds to a polymer with a defined number of repeating units. The distances between the signals correspond to the molecular weight of the repeating unit.

The degree of polymerization (DP) as well as the attached end groups can be determined by the following relationship.

$$\mathbf{M_{MALDI} = M_{endgroup\text{-}1} + M_{endgroup\text{-}2} + DP * M_{repeating\text{-}unit} + M_{cationization\text{-}agent\text{-}(Salt)}} \qquad (28)$$

Example: Poly(propylene glycol):

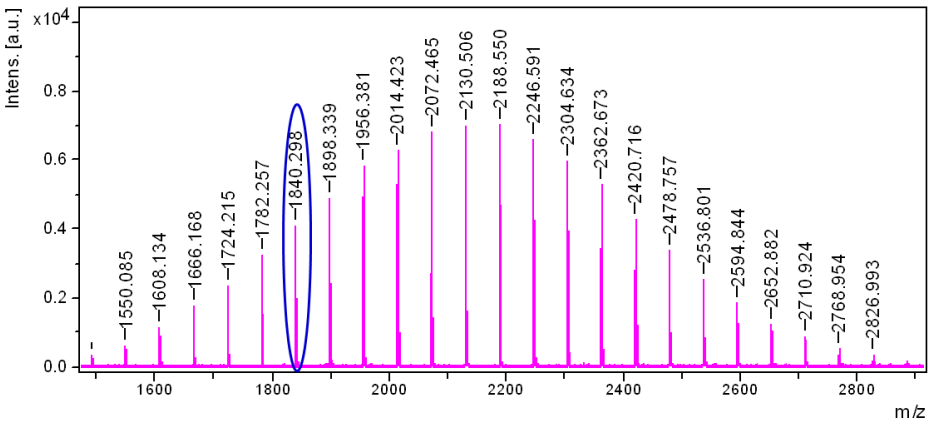

m/z	Resolution
1898.338	12099
1956.380	12557
2014.422	12568
2072.464	12810
2130.505	13192
2188.549	13579
2246.591	13817
2304.634	13611
2362.674	14322
2420.717	14377
2478.759	14986
2536.804	14965
2594.848	14785
2652.887	15486

Figure 22: MALDI-TOF Molecular weight distribution of a Poly(propylene glycol) sample.

Polypropylenglycol molecular formula: H-(-O-C_3H_6)$_n$-OH
Peak at 1840D
Repeating unit: OC_3H_6; $M_{repeating\text{-}unit}$= 58D
End group 1 = H; $M_{endgroup\text{-}1}$ = 1D
End group 2= OH; $M_{endgroup\text{-}2}$ = 17D
Cationisation-agent NaCl = Na^+; $M_{cationization\text{-}agent}$ = 23D
1840 = 1 + 17 + DP*58 + 23 → DP = 31

→1840D signal corresponds to a polypropylene glycol molecule with 31 propylene glycol units as well as one -H and one -OH end group.

In the low molecular weight range (up to 10000 Da), the signals are often isotopically resolved. In the area above 10000 Da no isotope resolution is obtained. Up to 20000 Da the signals of the individual polymers are still baseline separated and thus a discrete molecular weight distribution can be measured. In the area of high molecular weight, only continuous distributions can be measured. However, in rare cases, the spectrum can still be resolved to obtain resolution of repeat units. Jackson *et al.* investigated the difference between the determination of molecular masses via MALDI-TOF-MS and SEC. Reading this article is highly recommended. [1]

Further Readings:

H. Pasch, W. Schrepp, *MALDI-TOF Mass Spectrometry of Synthetic Polymers*, Springer Verlag, Berlin Heidelberg, **2003**.

Wilson & Wilson's, Comprehensive Analytical Chemistry, Elsevier, **2008**, *53*, 712ff.

[1] C. Jackson, B. Larsen, C. McEwen, *Anal. Chem.*, **1996**, *68*, 1303.

7. Fundamentals of Thermoanalysis (DSC, TGA)

One of the most important properties of polymers is their thermal behavior. Knowledge of thermal behavior is not only important for selecting suitable manufacturing processes, but also for the characterization of physical and mechanical properties, and of course for the choice of a polymer for a particular purpose. It is important to know the temperature-dependent properties of a polymer that are generally characterized by a glass transition temperature T_g and additionally by a melting temperature T_m in case of semicrystalline polymers. For semicrystalline polymers the melting point is more important especially for mechanical strength and processing. Furthermore, the temperature range within which the polymers are thermally stable is crucial for a specific application. By using thermogravimetric analysis (TGA) one can investigate the degradation behavior in addition to the thermal decomposition point.

7.1 Differential Scanning Calorimetry (DSC)

7.1.1 Glass transition temperature and melting point

Although many low molecular weight substances show a glass transition, this phenomenon is usually associated with polymers. The simplest definition of the glass transition temperature T_g is the following:

- Below T_g: The polymer is glassy.
- Above T_g: The polymer is rubbery.

This definition only applies to completely amorphous polymers. From a molecular point of view, the chain segments start to slip against each other above the glass transition temperature.

At low temperatures close to 0 K the atoms of a polymer chain are still able to probe small oscillations around fixed positions. If the temperature is increasing, the amplitude of these oscillations is increasing until finally the whole segment is completely mobilized. Above T_g, segments can perform cooperative rotations, translations and diffusion processes. When the temperature is sufficiently high and above T_g an amorphous polymer behaves like a highly

viscous liquid. The characteristic performance of a polymer depends strongly on the glass transition temperature. While polystyrene is brittle at room temperature, natural rubber (cis-polyisoprene) shows typical elastomeric properties. If one cools natural rubber to temperatures below its glass transition (-72 °C), it becomes rigid and brittle and can be shattered to pieces with a hammer. On the other hand, polystyrene is no longer brittle and shows typical elastomeric properties at temperatures above T_g. The T_g can be measured in various ways that not always lead to the same result. This reflects the kinetic and not the thermodynamic nature of this transformation, and also the fact that the T_g depends on the heating rate and the history of the polymer. Thus, the glass transition is not a 2^{nd} order transition in the strict sense; it is termed a pseudo-second order transition. The T_g can be measured with differential thermal analysis (DTA), by measurement of the temperature dependence of the refractive index or the dielectric constant, by dynamic mechanical analysis (DMA), by NMR measurements and some more techniques.

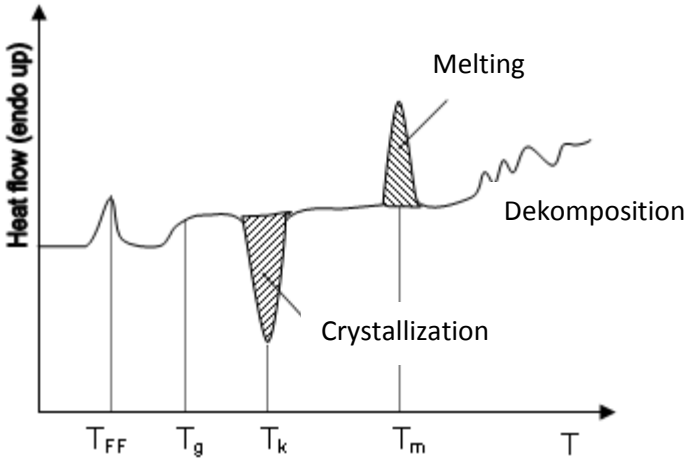

Figure 23: Example of a DSC curve. T_{FF} stands for a solid-solid transition.

For crystalline polymers, the melting point T_m is the most important thermal transition. The changes in the properties of a highly crystalline polymer at T_m are much more pronounced compared with those of amorphous polymers at T_g. The changes are characteristic for a thermodynamic 1^{st} order transition: A sudden change in heat capacity, volume, density, refractive index, birefringence, or in transparency is observed, or the occurrence of heat of fusion. Each of these variables can be used to determine T_m. In contrast to low molecular weight substances, melting and crystallization of polymers occurs over a wider temperature range: The exact melting point of each crystalline region depends on its size and quality. Large and perfect crystallites melt at a higher temperature. Since size and quality of the crystallites depend on the rate of crystallization and other factors, T_m depends to some extent on the thermal history of the samples. In some cases it is possible to bring the sample into an

amorphous state by rapid quenching with liquid nitrogen. **Figure 23** shows some characteristic signals caused by the thermal transitions described above.

7.1.2 Setup and measurement

This equation is used to determine the enthalpy of melting via DSC analysis.

$$\Delta H_m = \frac{K}{mq} \int_{T_i}^{T_f} \Delta T dT \tag{29}$$

ΔH_m	Enthalpy of melting per g polymer
q	Heating rate
K	Apparatus constant, determined by calibration
ΔT	Temperature difference/ energy difference between sample and reference
T_i, T_f	Start and Finish of conversion

According to the aforementioned equation an apparatus must be designed to fulfill the defined set of tasks. In **Figure 24** the principle of a DSC cell is shown schematically.

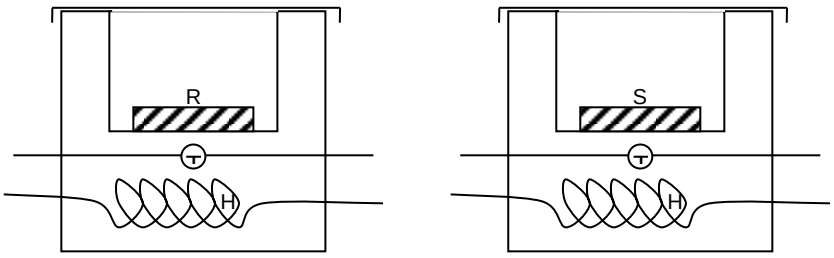

Figure 24: Schematic representation of the DSC sample head. S = sample, R = reference, T= temperature sensor, H = individual heating of the sample or reference.

In the DSC cell sample and reference are heated separately by individually controlled elements in a way that both always have the same temperature. A typical DSC plot uses the

difference in heat flow between reference and sample as the ordinate and the temperature as abscissa. The main difficulties arise from heat conduction problems. The latent heat of a 1st order transition, e.g. the enthalpy of fusion, is determined by integrating over the temperature range of the melting temperature (area below T_m peak). First, the DSC must be calibrated so that the internal units of the DSC can be converted into thermal units. Meaningful integration is only possible if a base line was subtracted from the curves before.

The DSC method is applicable for measuring transition temperatures, specific heats and heat quantities of transitions and reactions with non-volatile substances. The temperature range is about -100°C to 600°C. With accurately weighed samples an accuracy of about ± 2% in specific heats can be determined after careful calibration.

7.2 Thermogravimetric Analysis (TGA)

Thermogravimetric analysis measures temperature and/or time-dependent changes in mass of a sample. Typically, the technique is used to assess the thermal stability of a material and the decomposition temperature of a sample. Furthermore, TGA is a convenient method of verifying any modifications to materials or martial compositions. There are several associated standard methods for TGA measurements.

TGA experiments can be conducted either with a heating rate or in isothermal mode. When applying a heating rate, the sample is subjected to a controlled temperature program in a controlled atmosphere (N_2, air, etc.), and its mass is monitored. For this purpose the sample is put into an inert crucible (Al_2O_3) and heated at a constant heating rate (typically 5-20 K/min) normally up to 650°C. Alternatively, experiments can be performed isothermally and the mass change is recorded against time. In this case the sample is rapidly heated up to the requested temperature. Isothermal runs are useful for studying processes such as moisture absorption or desorption, curing reactions that produce small volatile molecules or to determine the specific stability of a material at a certain temperature (emission of HCl from PVC). Isothermal measurements are also more meaningful for certain applications that require constantly high temperatures, as practical conditions can best be approached.

The result of a TGA experiment is a thermogravimetric curve from which mass loss and associated temperature values can be extracted. A typical TGA curve is shown in **Figure 25**.

Based on the decomposition temperatures and the mass losses, the mechanism of decomposition of the whole material can be understood. Sometimes TGA is coupled with other analytical instruments, like IR spectrometers, or the exhaust is optionally separated by gas chromatography and later on analyzed by mass spectroscopy.

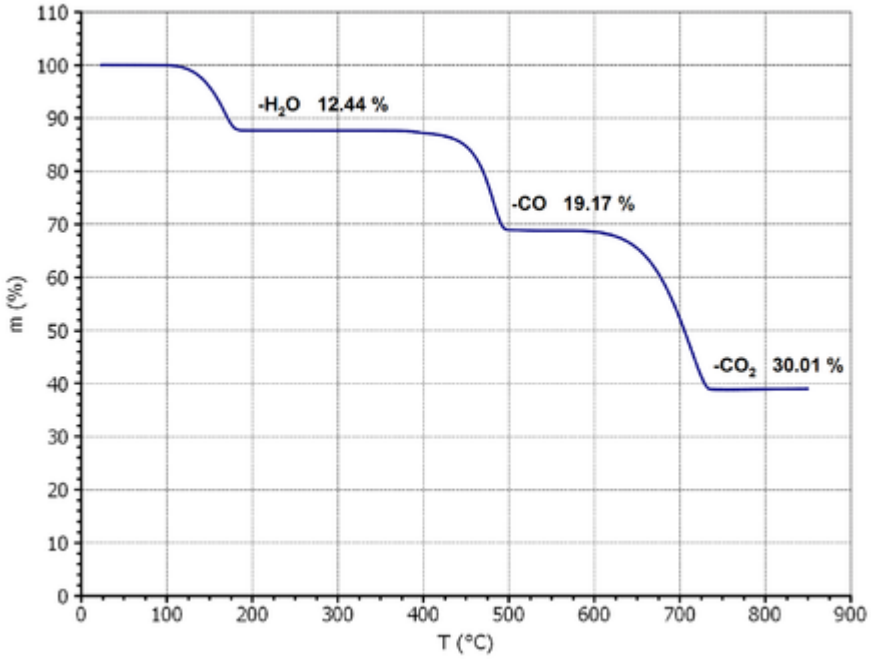

Figure 25[1]: TGA curve of calcium oxalate monohydrate. In the first step the water is removed. Secondly the oxalate is transferred into calcium carbonate and in the last step the carbonate is converted into calcium oxide.

[1] http://de.wikipedia.org/wiki/Thermogravimetrische_Analyse#mediaviewer/File:Calcium_oxalate_TGA_01b.png, 19.11.2014

8. Basic concepts of polymer processing

Plastics from macromolecules consisting of linear or branched chains only held together by intermolecular forces are known as thermoplastics. Some intermediate steps are required to transfer the crude thermoplastics produced in a chemical process to a product which is used by the consumer. Plastics are made in the form of granules, powders, pastes or as liquids, and then processed into semi-finished or finished products. Semi-finished products are intermediates which will be processed later on by different forming techniques to the final products. Examples of semi-finished products are plates, sheets, tubes and profiles made from plastic. Finished parts are made from processes like the injection molding processes. Examples of finished products are buckets, gears or plastic housing. Decent processing conditions and best product properties require a pre-treatment of the raw material before shaping. The treatment has two important tasks. First, additives which may be present in different amounts must be dispersed within the polymer homogenously, and on the other hand the raw material must be brought into a form (e.g. granules) which facilitates the processing.

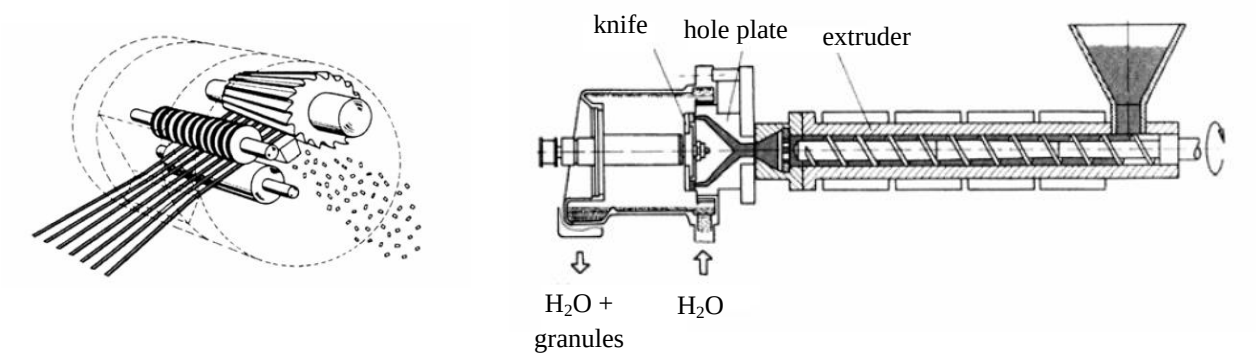

Figure 26: Cold granulation (left) and melt granulation (right).

Granulating means cutting plastic strands into small pieces (cf. **Figure 26**) There are two variants of the granulating or pelletizing process. Cold granulation means that the plastic is first cooled and then cut into pieces. The disadvantage of this procedure is that the pieces have burrs and therefore these particles trickle worse than hot granulated particles. In a hot pelletizing process the raw material is plasticized in an extruder, pressed through a simple perforated plate, and the extruded strands are cut by a knife. The resulting pieces are cooled by air or by water. This process leads to a more pourable granulate due to the absence of sharp edges.

8.1 Extrusion

Extrusion is the continuous production of endless semi-finished plastic products. The product range extends from simple semi-finished products such as pipes, sheets and films to complex profiles. A direct further processing step of the still-warm semi-finished products for example by blow molding or calendering is possible. Since the plastic is completely melted during extrusion and receives an entirely new form, this method is one of the primary shaping methods. The extruder is the common part of all extrusion systems and related procedures. The purpose of an extruder is to prepare a homogeneous melt and to press the melt into a mounted tool. An extruder consists of the components shown in **Figure 27**. The screw performs a variety of tasks such as feeding, conveying, melting and homogenization of the plastic and therefore it is the heart of an extruder. The most common screw is the so-called three-zone screw.

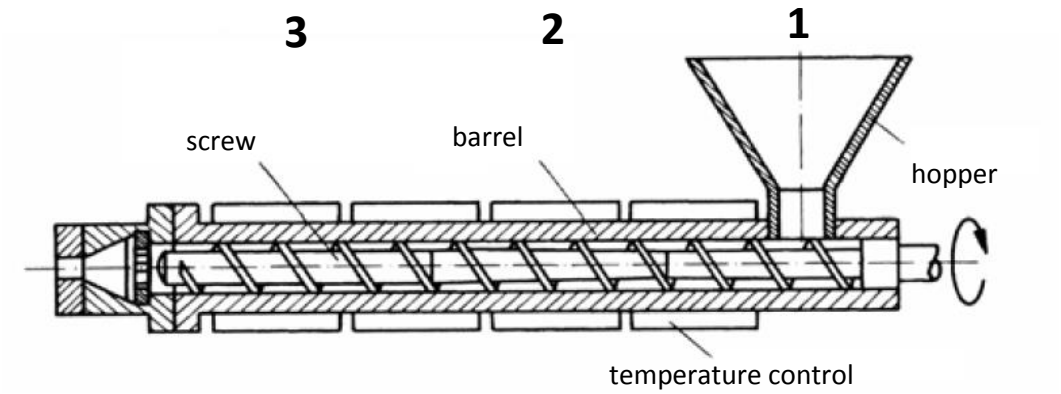

Figure 27: Schematic representation of a typical Extruder setup.

In the feed zone (1) the material is still solid. In the compression (2) zone the material is compressed and melted by the decreasing channel depth of the screw. In the metering zone (3), the molten material is homogenized and brought to the desired processing temperature. An important characteristic size of the screw is its length to diameter ratio. This ratio determines the performance of the extruder. Regardless of their design all screws must fulfill the following requirements:

- Production of a thermally and compositionally homogeneous melt
- Constant pulsation conveyance
- Processing of the material below its thermal, chemical and mechanical damage limits

From an economic perspective, a high mass flow rate is additionally involved besides low specific operating costs. These requirements can only be met if a good set of screw and

cylinder is present. Counter-rotating twin screw extruders are used for powdered materials and especially for PVC. The advantage of this extruder is that additives can be mixed into the material without strong mechanical or thermal stress. Thus, temperature-sensitive materials can be processed without being damaged.

The material melts in the extruder not only by friction, but also by heating the barrel. For this purpose, a temperature control system exists. The system is divided into several zones that can be heated or cooled separately. In the extrusion process materials are processed which can be used for injection molding, too. However, there is a great difference between the two methods. While during injection molding low viscosity and high fluidity are desirable, extrusion requires a high melt viscosity. The high viscosity ensures that the material is dimensionally stable. In the extruder the polymer is molten and mixed with additives. The mounted tool, which exhibits a flow channel, the so-called melt distribution manifold, dictates the shape of the extruded semi-finished product. The temperature of the tool can be controlled electrically to control the flow of the polymer melt and the cooling procedure. Usually, the melt is cooled down by air or water in order to be fixed in shape and dimension after leaving the tool.

Today, coextrusion processes are used to create materials for multilayer wire insulation, packaging films and extrusion blow molding. Such advanced procedures are necessary in case a single material is unable or too expensive to fulfill the tasks of a special application. Manufacturing of composites via coextrusion requires a separate extruder for each compound. In special coextrusion tools (cf. **Figure 28**) the melts are channelized separately and are combined just before leaving the tool and thus fused together. Nowadays, coextrusion can performed with up to seven independent extruders.

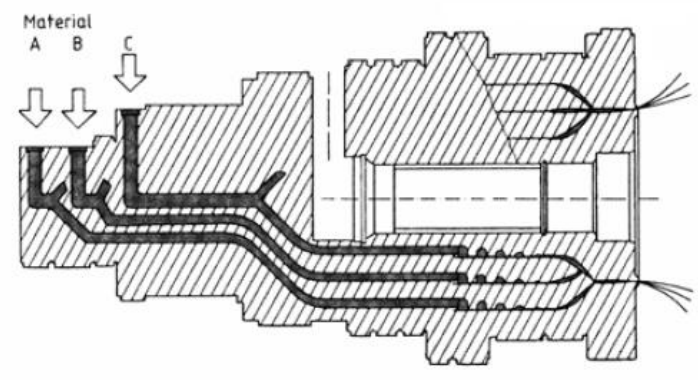

Figure 28: Coextrusion tool for three different compounds.

8.2 Injection molding

Injection molding is the most important process for the discontinuous production of molded plastic parts. About 60 % of all plastic processing machines are injection molding machines. Injection molding is one of the primary shaping methods, and products with weights from grams to kilograms can be made. In **Figure 29** the setup of an injection molding machine is presented.

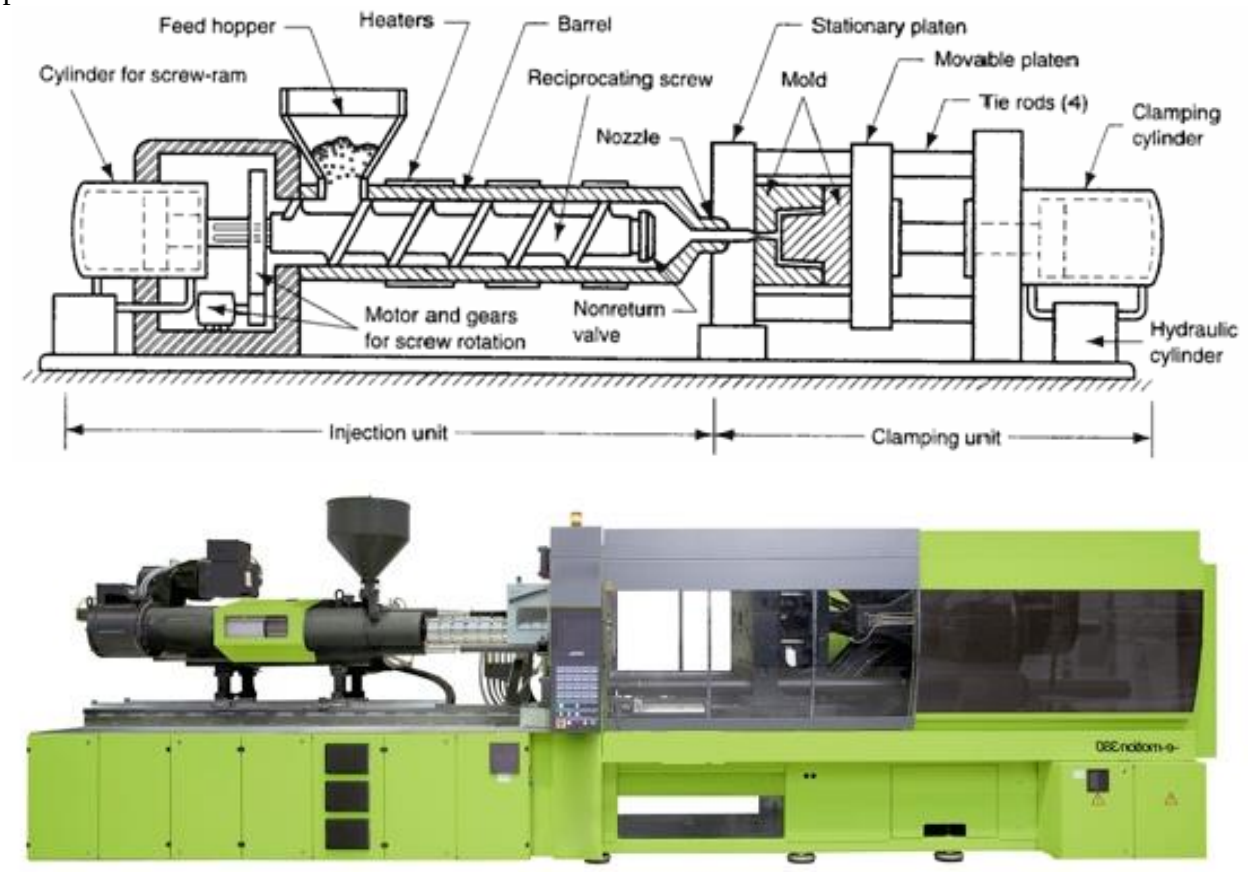

Figure 29[2,3]: Schematic representation of an injection molding machine (above); photograph of an injection molding machine (below).

In the injection unit the plastic is melted, homogenized, conveyed, dosed and injected into the tool. Today, it is common to use reciprocating screw injection molding machines. These injection molding machines are working with a screw which also serves as the injection plunger. This unit is very similar compared to an extruder. The injection unit is in general movably mounted on the machine table.

[2] http://www.xcentricmold.com/images/injection-molding-machine.gif

[3] http://www.kompack.info/www.kompack.info/Engel_K_Vorschau_files/droppedImage_3.jpg

Usually the barrels, screws and nozzles can be replaced so the machinery can be adapted to the material to be processed or to the volume of one shot. The clamping unit of an injection molding machine is comparable to a horizontal press. The nozzle-side clamping plate is fixed; the other side is designed in a way the components can be moved laterally. On these vertical platens, the tools are attached such that the finished molded parts fall down after ejection. The tool does not belong directly to the injection molding machine, as it is designed individually for each product. It consists of at least two main parts, wherein each part is attached to a backing plate of the clamping unit. The maximum tool size is specified by the size of the two platens and the distance between the two adjacent spars of the injection molding machine. The tool basically consists of the following elements:

- Mold plates with the cavity
- Gating system
- Temperature control
- Ejector

Generally, tools are very expensive, they cost from 5000 € up to several 100,000 €. This is the reason why only productions with a larger piece number are profitable. Injection molding is suitable for mass production because the materials can be converted into a finished part in mostly one operation step. In contrast to the metal casting or pressing of thermosets or elastomers, thermoplastic products can thus be produced by injection molding without burrs. Therefore, re-working of the products made by injection molding is negligible, and even complicated geometries can be made in one production step. Plastics which are processed using injection molding are usually thermoplastics, but also thermosets and elastomers can be processed. The output of parts per time unit is crucial for the economic feasibility of the process and depends strongly on the cooling time of the molded part. The cooling time in turn increases quadratically with the wall thickness of the molded product! This must be taken into account when molded parts with thick walls are to be produced. The time between the production of two parts is called cycle time. In **Figure 30** the injection molding process is shown schematically.

It can clearly be seen that the process steps are carried out sequentially. Only the important cooling process overlaps with other operations. These process steps are coordinated by the control device of the machine and are repeated with each cycle. The cycle time should be as low as possible in order to achieve a high throughput and a good efficiency of the process.

During the first step the material is conveyed from the hopper into the direction of the tool by the screw, which rotates in a barrel. Here, the material is compressed and melted.

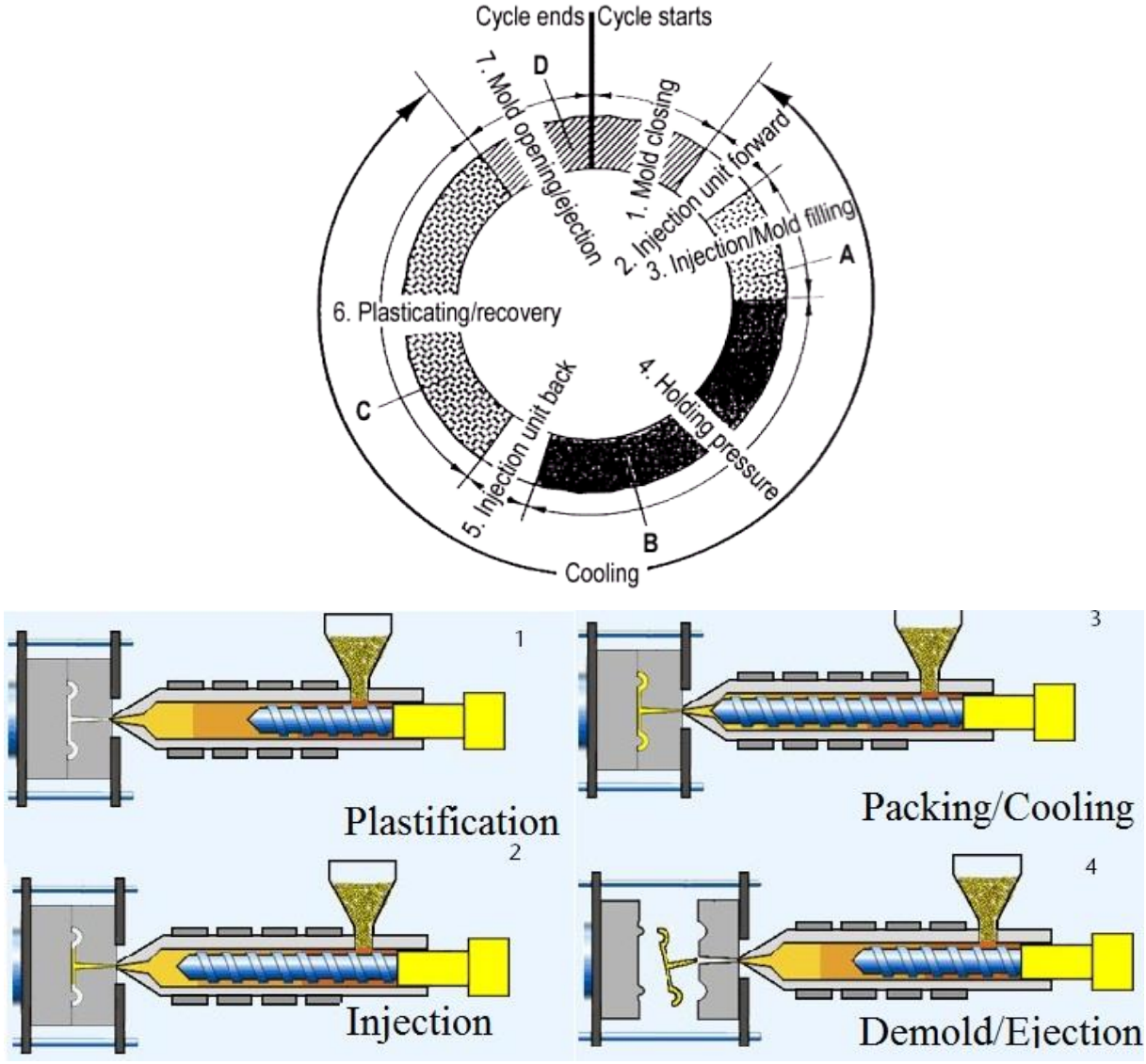

Figure 30[3,4]: Injection molding process.

During the conveying process, the material accumulates in front of the screw tip while the screw is simultaneously pushed back by the melt. The conveyance of the material is stopped when the screw has reached a certain position. At that time, enough material is gathered in front of the screw to be injected into the mold. The distance covered by the screw is called metering; the volume of the material in front of the screw is called metered volume. Both parameters have to be readjusted for each tool.

[3] https://www.tut.fi/ms/muo/tyreschool/moduulit/moduuli_6/hypertext/3/kuvat/pic3_3_2_thumb.gif

[4] http://www.intechopen.com/source/html/16394/media/image2.jpg

During injection, the screw moves forward without rotating, driven by the hydraulic injection barrel and pushes the metered melt through a nozzle into the mold. Due to the back flow valve the screw acts in this case as a piston. The injection pressure is set in the machine as a fixed parameter and represents an upper limit which cannot be exceeded.

Another variable which must be set is the injection speed which may be varied during injection. The flow processes in the tool can be divided into three phases:

- Phase 1 injection phase
- Phase 2 compression phase
- Phase 3 dwell pressure phase

During the injection phase the tool is filled volumetrically. Once filling is completed, and the compression within the tool begins. Further mass is still required to fill up the tool completely while compression takes place, which amounts to approximately 7 %. During the compression phase the pressure in the cavity rises steeply and at a predetermined pressure in the tool, the dwell pressure phase begins. Upon cooling, the material shrinks in the mold and new material has to be provided to keep the volume constant. This is the task of the dwell pressure phase. The pressure in the mold shrinks at constant pressure during the third phase, because the molded part solidifies more and more. Once the pressure has dropped to ambient pressure, the dwell pressure phase is completed. It is important to know when to switch to the dwell pressure phase. Too short times do not allow the precise reproduction of the shape of the mold, sink marks forms. If the compression phase is too long, overmolding occurs and the resulting burrs need to be removed in a post working step. After the dwell pressure phase is completed, the injection unit starts in the same time with the new dosage. The cooling time begins with the filling and ends with the ejection. This time span is set such that the molded part has a certain temperature and hence is dimensionally stable, which process is aided by cooling the mold.

8.3 Electrospinning

Electrospinning is a method that allows the generation of polymer (and other) fibers with diameters down to the nanometer length-scale (cf. **Figure 31**). It is widely used in polymer science to produce diverse fibrous devices such as filters, membranes, wound dressings and scaffolds for tissue engineering. Furthermore it is possible to incorporate a wide array of functional agents (drugs, nanoparticles, etc.) into the fibers via the electrospinning process thus enabling an even wider field of applications such as drug eluting devices.

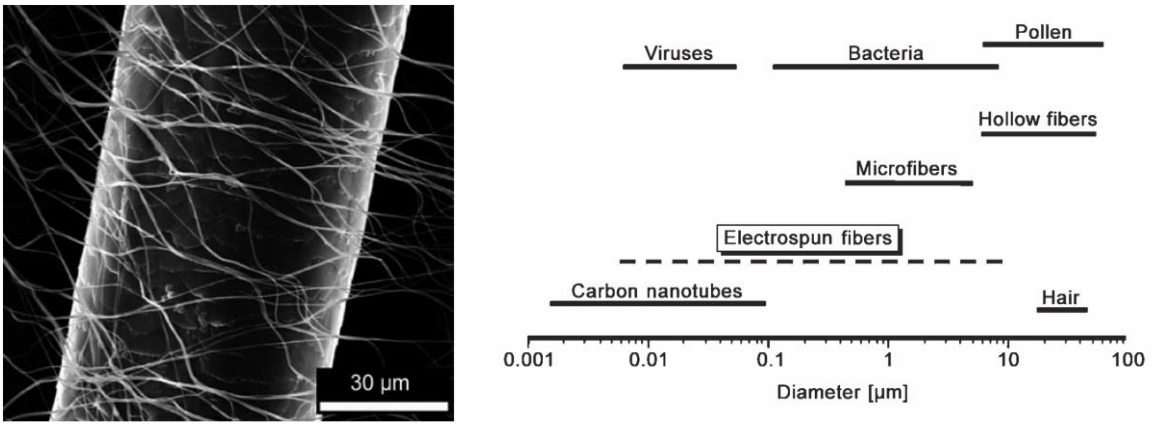

Figure 31: Left: Electrospun fibers of poly(vinyl alcohol) surrounding a human hair (SEM micrograph); Right: Length scale of electrospun fibers. (Reprinted from [1])

Electrospinning of polymers was first described in a patent from 1934 (A. Formhals, Mainz), however, it only gained wider attention in the 1990s. The process itself seems rather simple at first glance: A polymer solution or melt is transported through a thin metal nozzle (e.g. a syringe cannula) which is connected to high voltage generator and therefore constitutes an electrode. The counter electrode ("collector") can be of various geometries (planar, tubular, etc.) and is placed between 10 and 30 cm away from the nozzle. The voltage applied between nozzle and collector is in the range of 100-500 kV m^{-1} (with low currents in the microampere range) and results in the formation of a so-called Taylor cone at the drop of the polymer solution or melt (cf. **Figure 32**). At sufficiently high voltages, a jet is formed from the drop and accelerated towards the collector. In the course of covering the distance between nozzle and collector, the jet undergoes jet-thinning (becomes narrower), the solvent evaporates (or the melt solidifies) and solid polymer fibers with diameters ranging from micro- to nanometers are deposited on the collector.

However, the physics behind this method is very complex and the adjustment of the process parameters such as the molecular weight of the polymer, the concentration of the polymer solution, the solvent properties and the applied voltage are often difficult to handle. Even the ambient temperature and humidity can have a severe impact on the outcome of the electrospinning process.

Many synthetic and natural polymers have been electrospun into fibers and equally numerous are the fiber structures and morphologies that have been obtained by this process. Depending on the material and the process parameters the formed fibers can be perfectly circular or rather flat ribbons, exhibit a smooth surface or a porous structure and can be regularly shaped or exhibit beady defects. Extensions of the process are the application of special nozzles for the generation of core-shell fibers (coaxial electrospinning [2]) or the usage of emulsions as spinning solutions (emulsion electrospinning [3]).

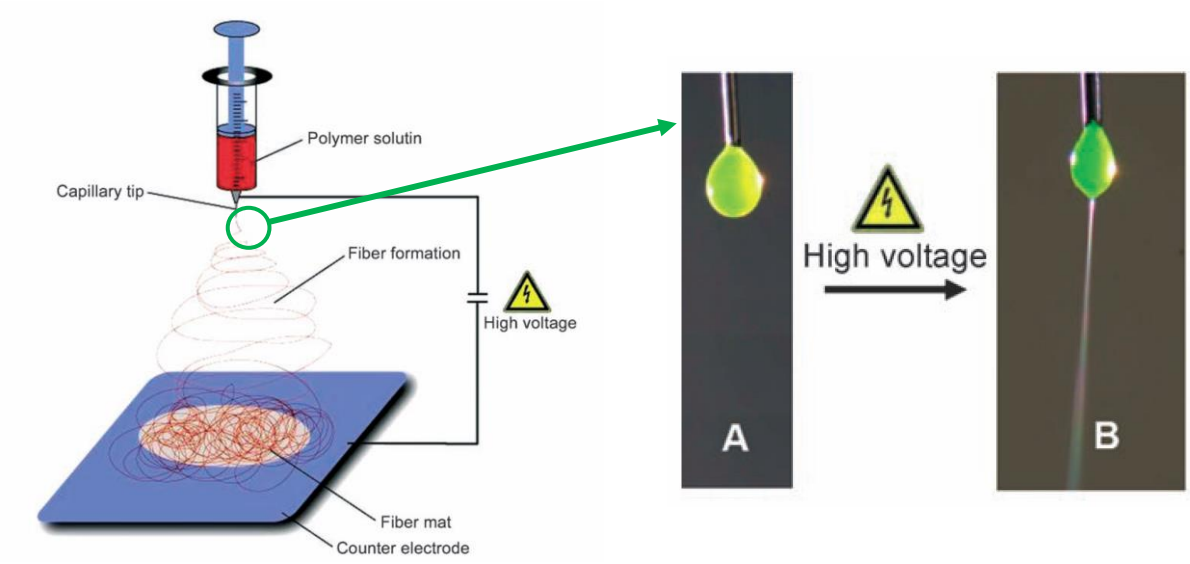

Figure 32: Left: Electrospinning setup; Right: a droplet of a polymer solution at the nozzle without an applied voltage (A) and with an applied voltage of 20 kV resulting in the formation of a Taylor cone and the emergence of a jet (B). (Reprinted from [1])

Bibliography and Further Readings:

[1] A. Greiner, J.H. Wendorff, *Angew. Chem. Int. Ed.*, **2007**, *46*, 5670.

A. Greiner, S. Agarwal, J.H. Wendorff, Electrospinning*: Materials, Processing, and Applications*, Wiley, **2012**.

[2] H. Jiang et al., *J. of Contr. Rel.* **2005**, *108*, 237.

[3] J.C. Sy, A.S. Klemm, V.P. Shastri, *Adv. Mater.* **2009**, *21*, 1814.

9. Introduction to rheology and mechanical testing

Rheology is the science of deformation and flow of matter. Generally all matter, not only liquids but also solids, flow. The main difference is the timescale of the flowing process. In theory there are the concepts of an ideal viscous Newtonian fluid and an ideal elastic Hookean solid. In reality most materials are viscoelastic, which means that their mechanical behavior lies somewhere in between. Because the scope of rheology is very large, e.g. polymer solutions, colloidal solutions, industrial paints and products from the food industry are characterized, we concentrate on the rheological behavior of molten thermoplastics (Note: Amorphous polymers below their glass transition temperature can be considered as undercooled melts.). As the name thermoplastic implies, the materials´ response to stress depends on temperature but also on the timescale of the experiment, as discussed below.

Newtonian Fluid

Newtonian fluids exhibit ideal viscous behavior. They are characterized by the property that the flow resistance is proportional to the flow rate. This means that the viscosity η of a liquid remains constant over the entire shear rate range $\dot{\gamma}$ during a shear experiment (cf. **Figure 32**). As a result, a linear relationship between the shear rate $\dot{\gamma}$ and the shear stress σ is obtained, which is described by the law of Newton:

$$\sigma = \eta \cdot \dot{\gamma} \tag{30}$$

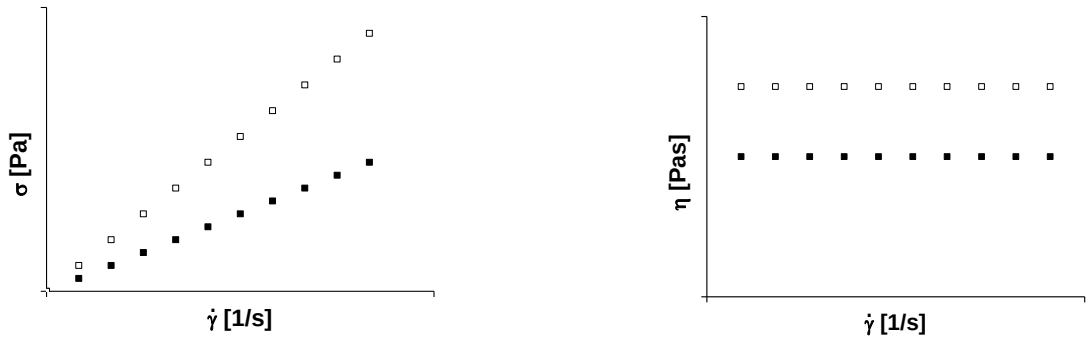

Figure 33: Flow and viscosity curve according to Newton.

The mechanical behavior of a Newtonian fluid can be described by the dashpot model (cf. **Figure 34**).

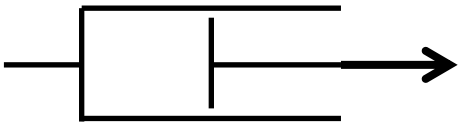

Figure 34: Dashpot model.

When applying a constant force, the piston displacement increases steadily, while the damper fluid flows through the narrow gap between the piston and the cylinder wall. Increasing piston speeds $\dot{\gamma}$ result in linearly increasing stresses σ. The proportionality factor, i.e. the resistance to flow, is called viscosity (s. Equation (30)). Fluids which show different behaviors are called non-Newtonian (see also thixotropy, rheopexy, dilatant, shear thinning).

Hookean Solid

Hookean solids exhibit ideal elastic behavior. The deformation behavior of an ideal elastic material is described by Hooke's law:

$$\sigma = G \cdot \gamma \tag{31}$$

The mechanical behavior of a Hookean solid can be described by the spring model (**Figure 35**).

Figure 35: Spring model.

By applying a constant tensile force the spring deforms almost instantaneously. The degree of deformation γ is proportional to the applied force σ. The proportionality factor G, the so-called modulus, corresponds to the stiffness of the spring.

Viscoelastic Materials

As mentioned before all real materials, including polymer melts, exhibit both viscous and elastic behavior, which is why they are called viscoelastic. From rheological measurements material parameters such as viscosity, elasticity or characteristic relaxation times can be determined. These macroscopic parameters correlate to the molecular scale and allow gaining insight into the microstructure of the material.

Maxwell model

The Maxwell model describes ideal viscoelastic liquids. It consists of a serially arranged dashpot with the viscosity η and a spring with the spring constant G (**Figure 36**).

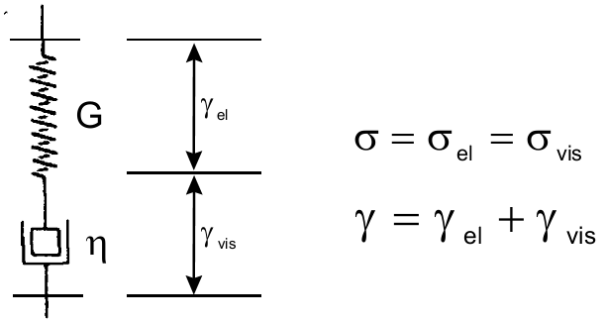

Figure 36: Maxwell model of an ideal viscoelastic liquid.

In the Maxwell model the stress of the spring σ_{el} and the dashpot σ_{vis} are equal, whereas the displacements (deformations) γ_{el} and γ_{vis} add up to the total deformation. According to the Maxwell model stress relaxation can be described by the following equation (for the derivation see textbooks):

$$G(t) = \frac{\sigma(t)}{\gamma(t)} = \frac{\sigma_0}{\gamma_0} e^{-t/\tau} = G e^{-t/\tau} \qquad (32)$$

The formula (32) describes the time dependence of the modulus during a stress relaxation experiment, as shown in **Figure 37**.

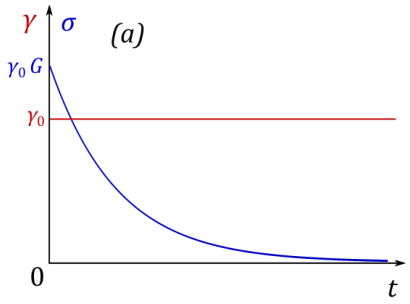

Figure 37: Stress relaxation experiment of an ideal viscoelastic liquid.

Voigt-Kelvin model

The Voigt-Kelvin model describes an ideal viscoelastic solid. It consists of a parallel aligned dashpot and spring (cf. **Figure 38**)

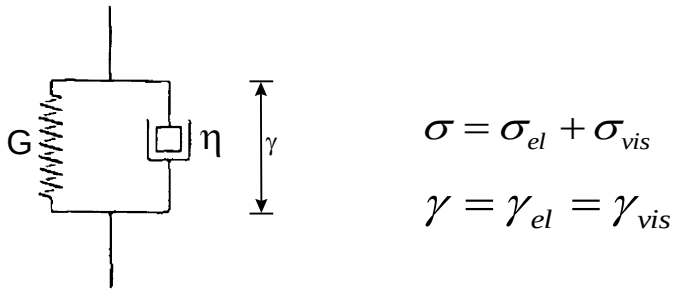

Figure 38: Voigt-Kelvin model of an ideal viscoelastic solid.

Here, the stress of the elastic and viscous contributions is added, whereas the displacements are the same. According to the Voigt-Kelvin model the creep experiment (cf. **Figure 39**) can be described by the following equation:

$$\gamma(t) = \frac{\sigma 0}{G}\left(1 - e^{-t/\tau_K}\right) \tag{33}$$

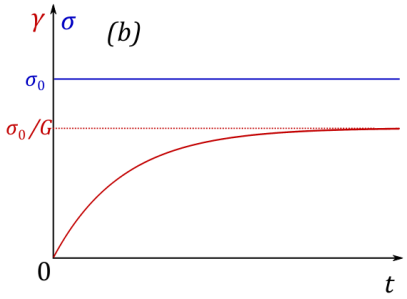

Figure 39: Creep experiment of an ideal viscoelastic solid.

Oscillatory shear Experiments (rheometry)

In this section the principle of an oscillatory shear experiment (cf. **Figure 40**) is described for a rheometer with plate-plate geometry, but it is also valid for other geometrical set-ups.

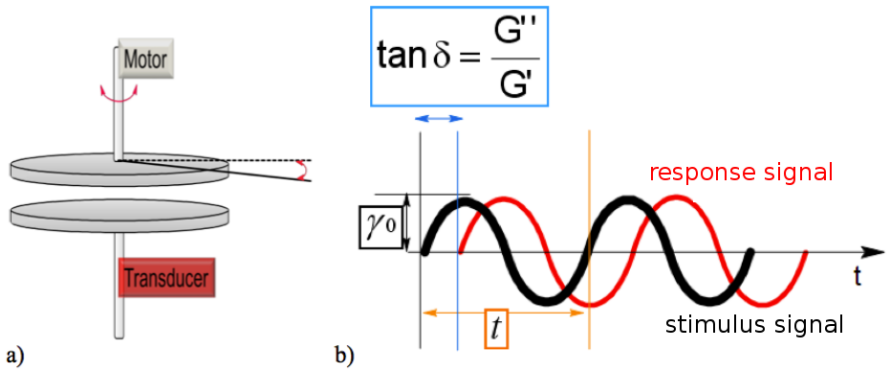

Figure 40: Oscillatory shear experiment.

If a viscoelastic material is sheared between two parallel plates with a sinusoidal excitation frequency from one plate, there will be a delay in time when the signal is detected on the other plate. This delay is the so called *loss angle* δ. The tangent of the loss angle is defined as the quotient between *loss* G'' and *storage modulus* G'. Loss and storage moduli are a measure for the stored or dissipated energy per volume. On the molecular scale energy is stored, when the molecules change their conformation reversible, whereas by slipping against each other energy is dissipated. The values for G' and G'' do not only depend on the microstructure of the material (e.g. molecular weight, entanglement, branching, intermolecular forces) but also on temperature and timescale (frequency). In general it is valid, that the higher the temperatures are the smaller are the moduli, which means more liquid-like behavior. On the other hand if a system has more time to relax between excitation and detection (e.g. by measuring at low frequencies) the more liquid-like the response will be. It is obvious that time and temperature can affect the material behavior in a similar manner, which is known as the *time-temperature superposition principle*.

To characterize a material master curves can be drawn. An example is shown in **Figure 41**.

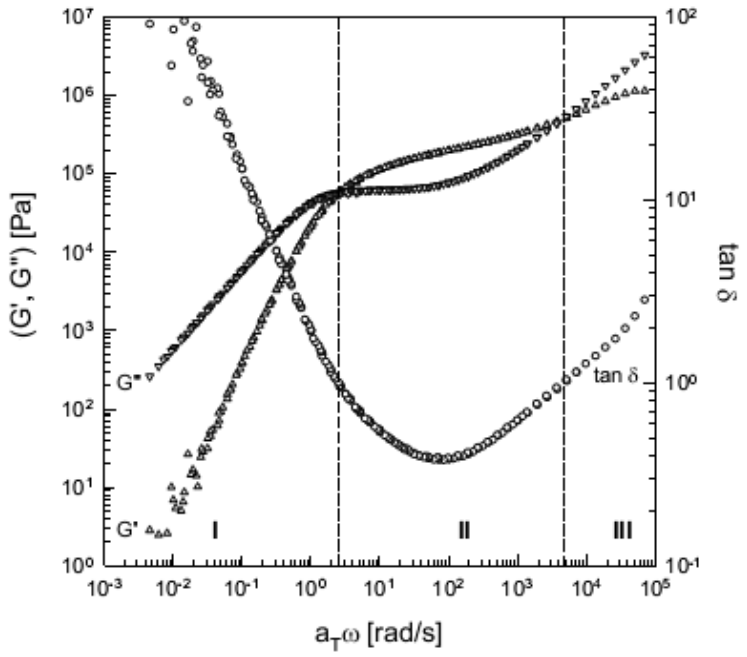

Figure 41: Master curve of a thermorheologically simple material with I: flow regime (with terminal regime where the slopes become 1 for G' and 2 for G''), II: plateau regime, III: glass transition regime.

As can be seen in Figure 41 the frequency range of the master curve is quite large which usually means it partially lies beyond the scope of a rheometer or in case of low frequencies the measuring time would be very long. To avoid these problems measurements are usually done in a narrow frequency range but at different temperatures. By using the time temperature superposition principle the curves obtained at different temperatures can be shifted and merged to one master curve. From the master curve we can get different characterisitc values like the terminal relaxation time τ_d and the entanglement molecular weight M_e. The terminal relaxation time, which can be seen as the time a chain segment needs to reptate out of its original tube (between two entanglement points), can be extracted by extrapolating the slopes of G' and G'' in the terminal regime and finding the intersection point. The entanglement molecular weight M_e can be derived by the so called plateau modulus. The plateau modulus G_n^0 is the value of G' in the plateau regime, where tan δ has its minimum. The following equation gives the relation between plateau modulus and entanglement molar mass:

$$G_N^0 = \frac{\rho \cdot R \cdot T}{M_e} \tag{34}$$

In this equation ρ is the polymer density, R is the universal gas constant and T is the temperature.

The dynamic viscosity η' can be derived from the loss modulus by following equation:

$$\eta' = \frac{G''}{\omega}$$

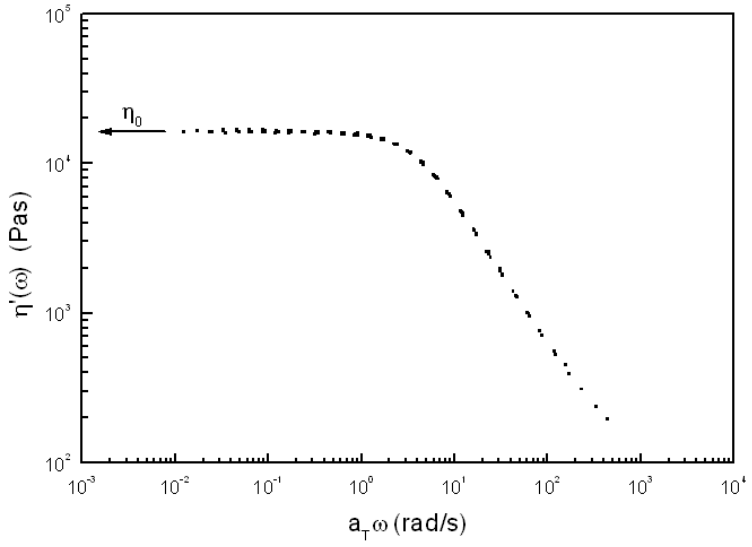

Figure 42: Frequency dependence of the dynamic viscosity.

By extrapolating the dynamic viscosity to zero frequencies we can get the zero shear viscosity η_0 (cf. **Figure 42**). For polymer melts there is an important dependence between zero shear viscosity and molecular weight:

$$\eta_0 = K \cdot M^{\alpha} \tag{35}$$

$$\alpha \approx 1, \text{ if } M \leq M_c \tag{36}$$

$$\alpha \approx 3{,}4, \text{ if } M \geq M_c \tag{37}$$

The shown equation is analog to the Mark-Houwink-equation, which holds for polymer solutions, but it´s not the same. M_c stands for critical molecular weight and is approximately two times the entanglement molecular weight. K is a material specific constant.

References and Further Readings

S. Bodendorfer, C. Gillig, S. Steinmann, Prof. Dr. Dr. C. Friedrich, *Grundpraktikum Makromolekulare Chemie - Rheologie"*, Universität Freiburg, **2014**.

S. Koltzenburg, M. Maskos, O. Nuyken, *Polymere*, 1st ed, Springer Spektrum, **2014**.

T. G. Mezger, *Das Rheologie Handbuch*, 3rd ed, Vincentz Network GmbH Co. KG, **2010**.

10. Microscopy of Polymer Systems

Microscopes open up doors to inspiring new worlds and have enabled major breakthrough discoveries. They are among the widest spread instruments in research and development and there is a great magnitude of different types of microscopes. This microscopy section however, is restricted to scanning electron microscopy (SEM), transmission electron microscopy (TEM) and on atomic force microscopy (AFM), which are frequently used for the characterization of polymer systems.

Microscopes are used to reveal the architecture of objects which are beyond the resolution capacity of the human eye. The naked eye can maximally distinguish points that are approximately 0.1 to 0.2 mm apart from each other. If we decrease this distance, we would only see one point. Using a light microscope (LM) at maximal magnification, we can nowadays distinguish points that are less than one micrometer apart from each other. For comparison, a human hair is approximately 100 µm in diameter. However, at this point the resolution limit of optical microscopy, known as the Abbe-limit, is reached:

$$d = 0.61 \frac{\lambda}{NA} \tag{38}$$

The minimal distance d between two points to be distinguished is defined by the numerical aperture (NA; 1.3-1.4 for modern objectives) and the wavelength λ of the employed light. The bottle neck for resolution is not the microscope but the wave length, which for light microscopes ranges from approximately 450 to 750 nm (UV-VIS). The understanding of this limiting factor spurred the development of electron microscopes in the 1930s. Using wavelengths thousands of times shorter than visible light, transmission electron light microscopes suddenly grant us access to the sub-nanometer range (~0.05 nm). This means we can visualize single molecules and even atoms! (cf. **Figure 43**)

With the invention of scanning tunneling microscopy (STM) in 1981 a new branch of microscopy was formed, called scanning probe microscopy (SPM). Instead of using electromagnetic irradiation (UV-VIS, or accelerated electrons) in SPM a specimen surface is physically probed. In the case of atomic force microscopy (AFM), a very sharp tip is rasterized over a sample surface to reveal its surface topography and even map its mechanical properties. Depending on the setup, SPM can reach atomic resolution, which is largely based on ultra-precise probe movements controlled by piezoelectric actuators.

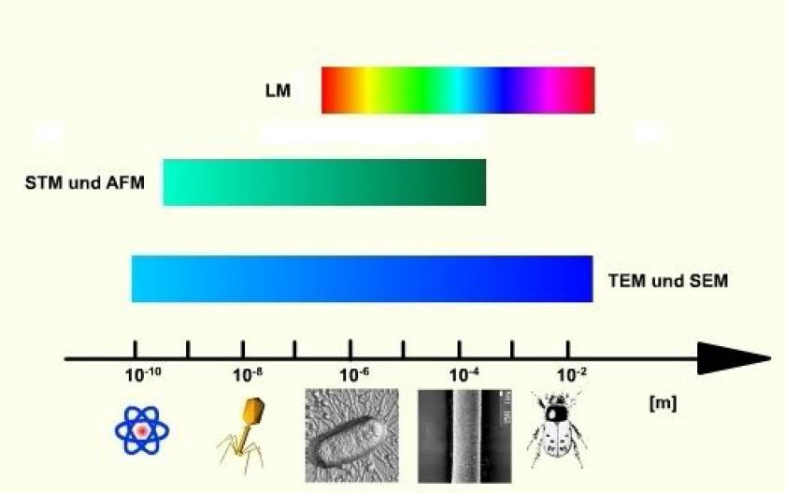

Figure 43: Magnification range of different microscopic techniques. Light microscopy (LM). Scanning tunneling microscopy (STM) and atomic force microscopy (AFM) are both scanning probe microscopy methods. Scanning electron microscopy (SEM) and transmission electron scanning microscopy (TEM). Below the scale are structures that can be visualized using with the corresponding microscopes. From left to right: single atom, virus, microbe, human hair, insect.

Electron Microscopy (EM)

In optical microscopy the light source can be for example a UV or a halogen lamp, a diode or a laser. All of them emit photons for specimen illumination. In contrast, EM uses accelerated electrons for sample irradiation. Since electrons are very small and easily deflected by hydrocarbons or gas molecules electron microscopes generally have to be operated under high vacuum. We have also mentioned that accelerated electrons have much lower wavelength, thus permitting for increased resolution but how can they be generated? First they are emitted from an electron gun through thermo-ionic emission. Similar to a light bulb, an electron gun contains a filament. This filament (cathode) is made up of tungsten wire and heated up by a small emission current to thermally release electrons. The emitted electrons are trapped inside the cathode cap (slightly more negatively charged than the filament) where they form an electron cloud. The anode below the cathode cap is electrically grounded and thus creates a positive attraction force accelerating the electrons trapped inside the cathode cap out through the small hole in the anode (see **Figure 44**, left). The voltage applied on cathode cap determines the energy of the accelerated electrons and thus their resulting wavelength. As mentioned before: The higher the voltage is, the shorter the wavelength and thus the higher

the theoretical resolution. However, at higher energy the electrons also create more damage to the sample.

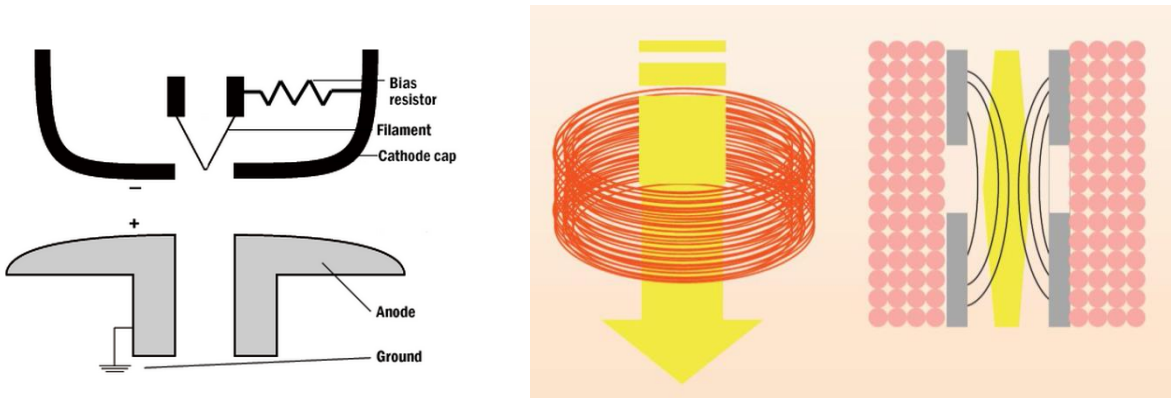

Figure 44: Schematic depictions of EM illumination source and an electron focusing element. Left: Electrons are released from a tungsten filament (cathode) and trapped inside the slightly more negatively charged cathode cap before they are accelerated by a positively charged anode. Right: Electromagnetic lens. Depending on the current applied on the copper wire solenoid, a magnetic field is generated (indicated by the filed lines) to focus the accelerated electrons (yellow arrow).

Whereas optical microscopes focus photons by means of glass lenses, these optical elements are opaque to accelerated electrons. Instead EM employs electromagnetic lenses (see Figure 44, right) which mainly consist of densely coiled up copper wire. Applying a current through this solenoid induces a radially symmetric magnetic field. Within this magnetic field accelerated electrons can be focused and the strength of the current determines the refractive effect of the electromagnetic lens. These accelerated electrons eventually collide with the atoms of a sample (generally solids) where they undergo different types of physical interactions (cf. **Figure 45**). Understanding the basic principles of these interactions will allow you to better understand the differences between SEM and TEM.

Transmitted electrons can entirely pass through an atom either without any deflection or with some deflection upon elastic collision. The latter is referred to as forward scattering and serves as the main signal for TEM. However, this works only for thin specimens and for carbon based materials. The maximal thickness is around 100 nm. Contrastingly, SEM detects electrons that are either reflected from or back-scattered out of the specimen volume by elastic collisions with the specimen atoms.

Yet another mode of interaction is an inelastic collision with an electron from the observed specimen. This leads to the ejection of a secondary electron (back-scattered) which is accompanied by the emission of characteristic photon (X-Ray). Such photons can be analyzed by X-ray photoelectron spectroscopy (XPS). XPS is a very sensitive surface (penetration depth max. is about 10 nm) spectroscopy technique to analyze the elemental/chemical composition of a specimen and can be combined with both, TEM and SEM.

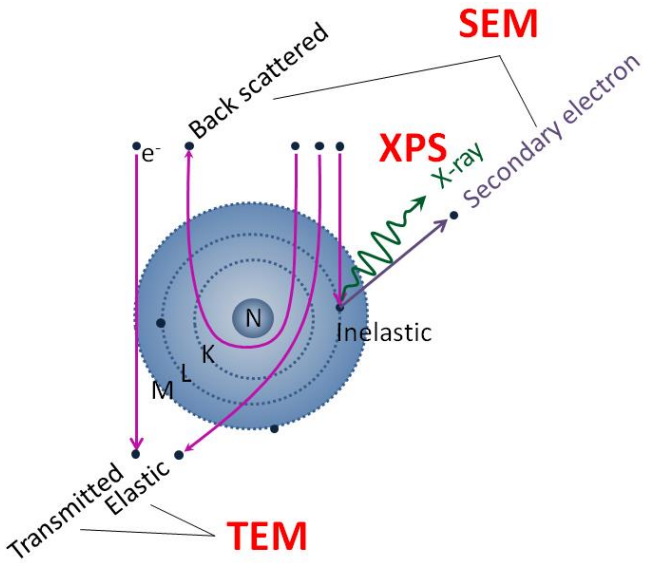

Figure 45: Schematic depiction of how an electron beam may interact with a sample with nucleus N, and electron cloud of electron shells K, L, M, showing transmitted electrons and elastic/inelastically scattered electrons. SE is a secondary electron ejected by the beam electron, accompanied by the emission of a characteristic photon (X-Ray) γ. BSE is a back-scattered electron, an electron which is scattered backwards instead of being transmitted through the sample.

Transmission Electron Microscopy (TEM)

Scope: As it can be seen in **Figure 46** (middle), the TEM configuration is very similar to optical light microscopy (Figure 46, left). Yet, TEM offers much greater resolution owing to the short wavelength of the electromagnetic irradiation (accelerated electrons instead of light) employed for sample irradiation. The theoretical resolution of TEM is around 0.05 nm which permits the observation of ultrastructural architectures in extremely thin (< 100 nm) samples. In our actual set-up at the Centre for Neurosciences (ZNF, cf. **Figure 47**) the acceleration voltage ranges from 60-120 kV and a point-to point resolution of ~0.4 nm can be achieved.

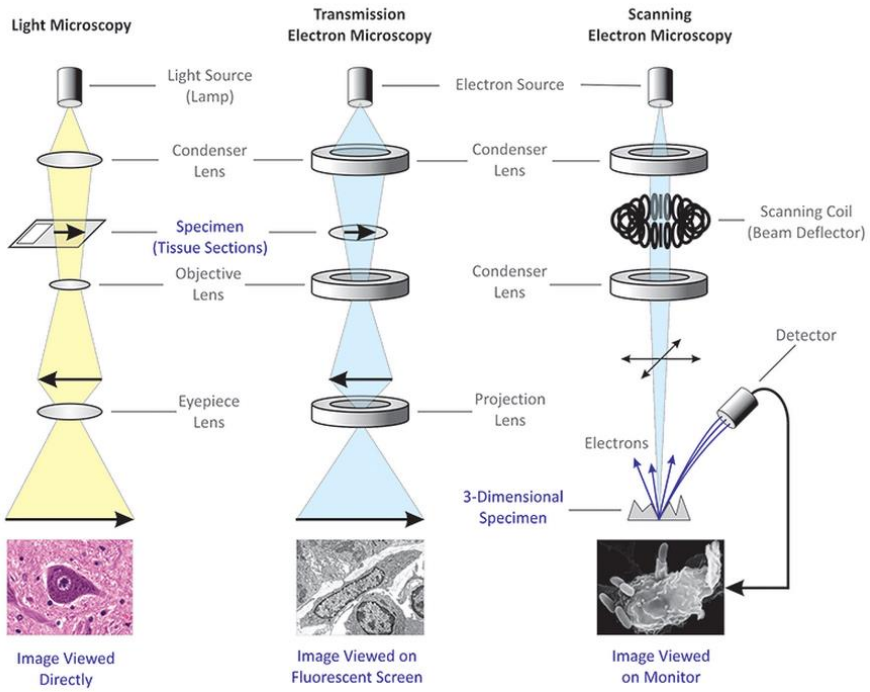

Figure 46: Schematic depiction of different microscopy modes. Left: Light microscopy (LM) Middle: Transmission Electron Microscopy (TEM). Note the very similar setup of LM and TEM. Right: Scanning electron microscopy (SEM). Here the detector is above the sample. The bottom row shows characteristic images for each modality. Note that the SEM allows for a very great depth of view.

Contrast: There are different modes of contrast in TEM but the most common one is bright field. Without the sample, the image is bright, thus the name. Introducing a sample leads to occlusion. The thicker the sample or the higher the atomic number, the darker the image will be. In dark field, the image without the sample is dark. Placing different apertures in the back focal plane enables the selection/exclusion of specific reflections (i.e. Bragg scattering). If the reflections do not include the unscattered beam, the resulting image will be dark where there is no sample. In case of a crystalline sample the electrons will be diffracted in characteristic patterns. From these patterns information about the crystal lattice geometry can be derived. Still another mode is the electron energy loss spectroscopy (EELS). As electrons pass through the sample they lose energy. The energy loss is characteristic for the elemental composition and can be detected by EELS. The resolution of the obtained images is lower than in bright field but therefore also contains information about the sample composition.

Polymers often have relatively low inherent contrast. This can be changed by staining the samples with solutions of heavy metals. In case of positive contrast, OsO_4 (selective for double bonds) and RuO_4 (selective for aromatic systems) only a specific phase of the sample will be stained and thus will show enhanced contrast (appears dark). For negative staining, the

heavy metal salt uranyl acetate assembles around the structure that is to be imaged. This is often done for particles. This way, the particles appear as bright spots in a dark matrix.

Figure 47: Zeiss LO 912 OMEGA TEM set-up at the ZNF.

Detector: The transmitted electrons are visualized by means of a phosphorescent screen (allows for direct observation by eye), photographic film or a sensor as i.e. a CCD camera. Of course the EELS mentioned above also serves as a detector to analyze the chemical composition of the sample.

Sample Preparation: Samples for TEM should not exceed a thickness of 200 nm but ideally they are < 100 nm. This can be achieved by different means. Using a microtome with a special diamond knife, samples can be cut into sections less than 100 nm in thickness. Amorphous polymers like polystyrene can be cut at room temperature (RT). However, polymers with a glass transition temperature T_g < RT have to be prepared in a cryo-microtome (typically at –120°C). Another method is spin coating, whereby thin films (around 50 nm) can be created by dropping a polymer solution onto a fast rotating disc. It is noteworthy, that the morphology of such spin coated discs may be different from macroscopic samples. Eventually, the film samples are placed onto small copper grids to insert them into the TEM. In case of nanoparticles (NP), a drop of NP suspension can be directly added onto the copper grid (with a carbon film).

A sample that is initially too thick for TEM, can also be thinned by means of an high energy ion beam. While this works well for inorganic materials this process generally leaves substantial artefacts in polymers. However, using a focused ion-beam (Ga-ions) a thin, free standing membrane can be carved out of a macroscopic sample. Although, this is a tedious process it often most successful for inorganic or polymer/inorganic samples.

Scanning Electron Microscopy (SEM)

Scope: SEM uses a focused electron beam (see Figure 46, right), which scans the sample in a raster like fashion. Typical energies range from 0.2 keV to 40 keV. The elctron beam is focused by one or two condenser lenses to a spot of approximately 0.4 to 5 nm in diameter. Another lens (deflector coil) moves the beam in the x- and y-axis. At each raster position a signal is collected. This ultimately produces an image of the sample´s surface topography with a great depth of view. The SEM at the ZNF (cf. **Figure 48**) can achieve a resolution of 1 to 1.5 nm, operates under high or low vacuum. The latter is the case in environmental SEM which is employed with materials that are not metal sputtered and or that may release gases.

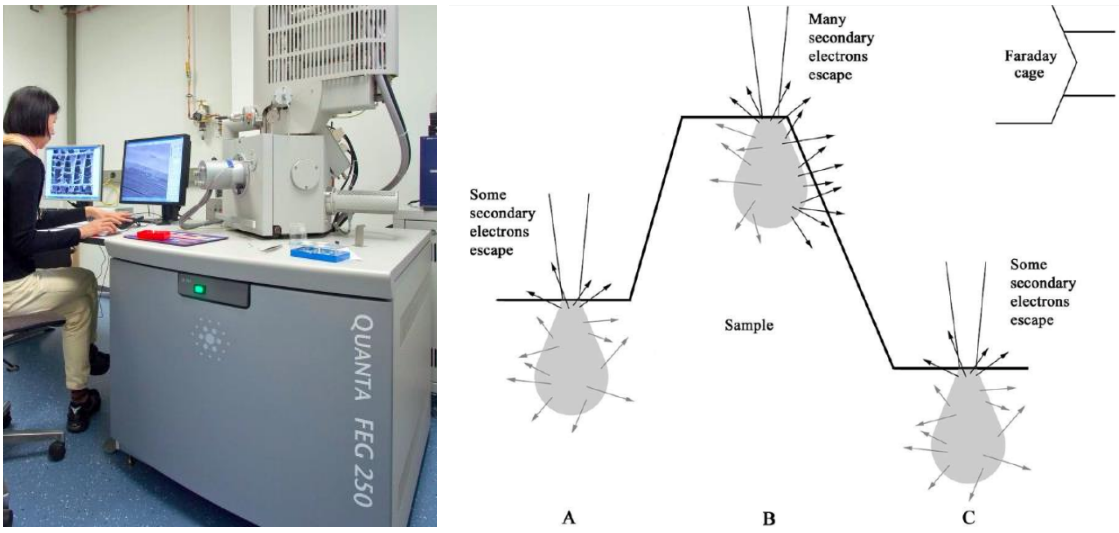

Figure 48: SEM setup and secondary electron detection. Left: Photograph of QUANTA FEG 250 SEM set-up at the ZNF. Right: Schematic depiction of secondary electron detection with respect to sample topography.

Contrast The most common signal source in SEM is based on secondary electrons (Figure 45 & Figure 48, right). Accelerated electrons induce the emission of secondary electrons through inelastic collisions with the atoms in the sample. From the site of impact on the sample, the secondary electrons evolve in a plume-like shape into the sample volume. The depth depends on the energy of the incoming electron beam and on the atomic number of the scattering sample atoms. For carbon rich samples, the plume can extend into the material more than 1 µm in depth. Depending on the topography these secondary electrons can again escape from the material to be collected by a detector that is placed above (or behind) the sample. Figure 48 (right side) demonstrates the amount of secondary electrons that can escape in three simplified scenarios (three different scanning points). Point A shows a flat raster point. Most of the secondary electrons dissipate into the sample and those who can escape, are blocked by

the hill-like sample structure at point B. At this hill-like raster point however, more secondary electrons can be collected since their escape through the side walls of the hill (facing the detector) is facilitated. Point C is again similar to point A but since there is no obstructive structure between this raster point and the detector, more secondary electron can be detected than in A. This way the sample is rasterized bit by bit by the electron beam and thereby reveals its surface topography.

Detector The Everhart-Thornley-Detector (ETD, cf. **Figure 49**) detector consists primarily of a scintillator inside a Faraday cage inside the specimen chamber of the microscope. A low positive voltage is applied to the Faraday cage to attract the relatively low energy (less than 50 eVs by definition) secondary electrons. Other electrons within the specimen chamber are not attracted by this low voltage and will only reach the detector if their direction of travel takes them to it. At the scintillator the electrons are converted into photons, which in turn are heavily amplified in the photomultiplier tube and eventually converted into a signal current. The SEM can also be fitted with an energy-dispersive spectrometer (EDX) to determine elemental analysis and for chemical characterization of the sample.

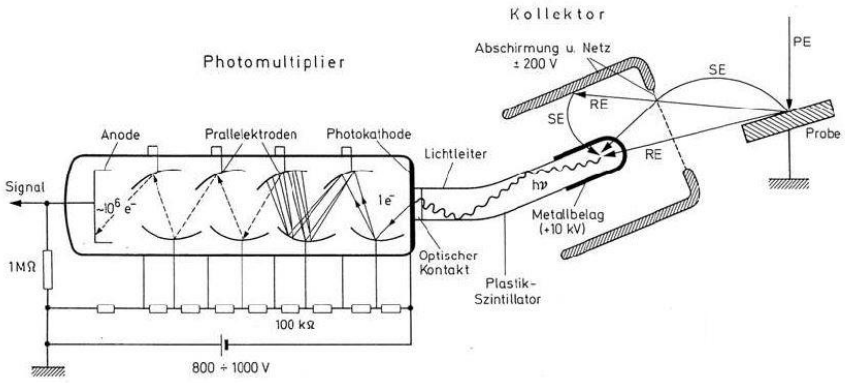

Figure 49: Schematic of the Everhart-Thornley Detector (ETD). Backscattered secondary electrons (SE) are converted into photons (hν) and ultimately a signal current is generated.

Sample Preparation For conventional imaging, the sample has to be electrically conductive and grounded. Otherwise, the sample becomes electrostatically charged, which leads to imaging artefacts. This is generally achieved by coating (sputtering) the sample with a few nanometer thick layer of metal as for example gold.

Atomic Force Microscopy (AFM)

In the 1980s, scanning probe microscopy (SPM) was introduced as an entirely new microscopy branch. The atomic force microscope (AFM) was invented in 1986 by Binnig, Quate and Gerber. Its principle is derived from the former scanning tunneling microscope (STM) developed by Gerd Binnig and Heinrich Rohrer from IBM, in Zurich who received the physics Nobel Prize in the same year. A few years later the first commercial devices were available. Nowadays, the market is led by companies like Bruker, Veeco or Agilent. The main purpose of the AFM is to take images of surfaces and to record information on sample topography. Recent advances in the field have led to increase the resolution to levels of a few angstroms and thus even enable image acquisition of single molecules (cf. **Figure 50**).

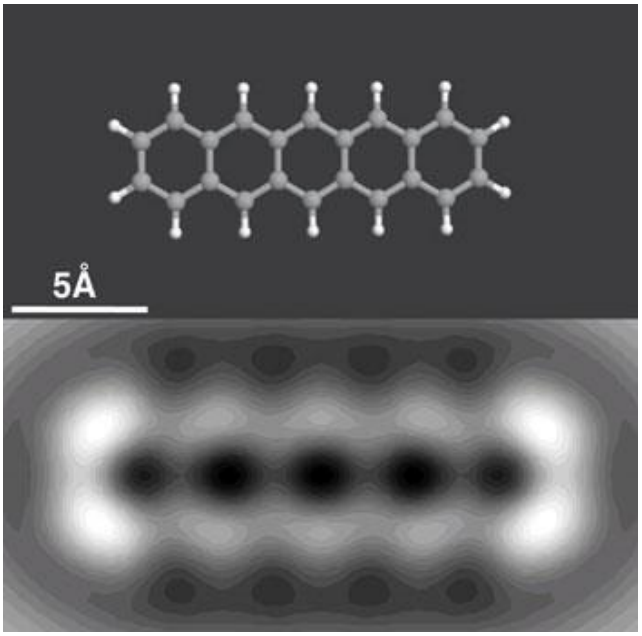

Figure 50: Ball and stick model of pentacene (above) and AFM (non-contact mode) image of pentacene on a copper surface (below). (Science/IBM Research – Zurich)

Advantages of the AFM over other microscopy techniques are the ease of sample preparation, the possibility of imaging in different environments (i.e. in liquids) as well as the acquisition of three-dimensional images, without needing special sample preparation. Also, the AFM is the only microscope with the ability to probe mechanical properties of a sample (i.e. attraction/repulsion force map).

As such, the AFM is a very versatile microscope and is used in many different disciplines as i.e. in physics, chemistry as well as in biology. In physics, it can be used to record images of atoms or to do nanolithography. Special modes are also used to move atoms and build nano-

scale devices. In biology, it is used to acquire images of living organisms under physical conditions. In the field of polymers and macromolecules, AFM is often employed to study the nanostructure (i.e. phase separation) of a material surface. It is possible to obtain a fine map of the topography of a solid polymer. From that it is also possible to measure different feature sizes or to determine the roughness of a sample.

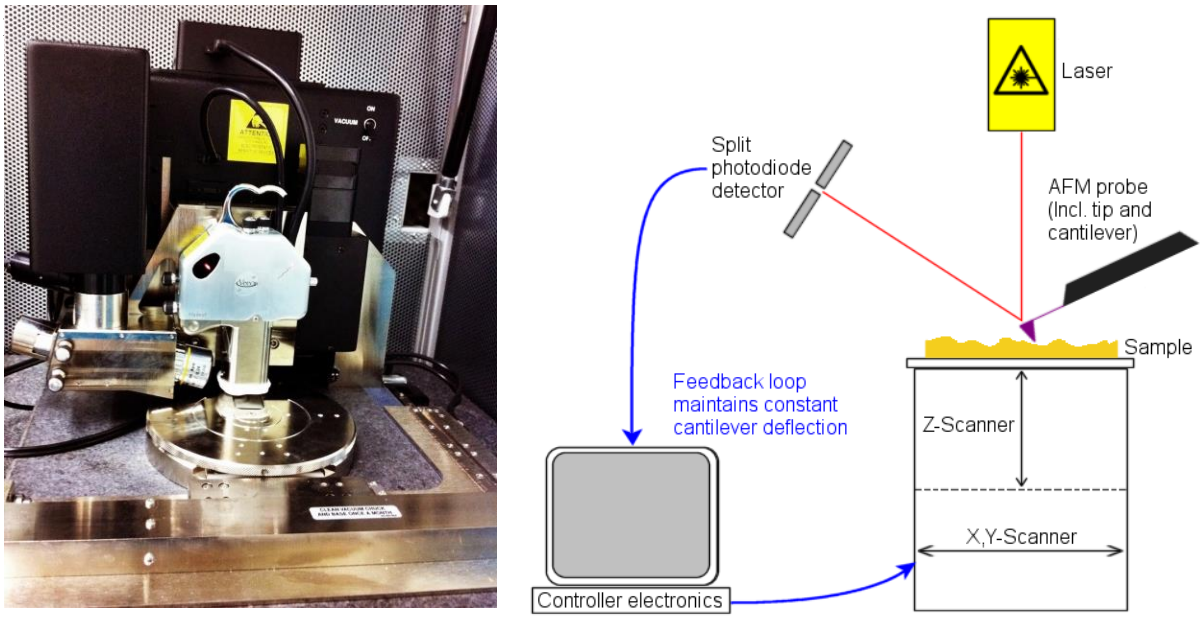

Figure 51: Photograph (left, Veeco instrument at the Shastri Lab) and schematic drawing of an AFM (right).

Probe: The probing part of the AFM is the cantilever tip which is etched out of a silicon or silicon nitride chip (see **Figure 51**, left). Generally, the very end of the tip is only a few atoms in size (around 15 nm in diameter). This tip literally feels surface of the sample as it is rasterized over the sample surface. The tip protrudes from the cantilever which, based on its geometry (triangle or bar shaped) or length, can have different spring constants. There is often several different cantilevers on one and the same chip and the spring constants can range from 0.01 to 40 N/m.

Probe/Sample Interaction: The Lennard-Jones potential (see **Figure 52**, right) can be used to describe physical interactions between the AFM tip and the sample depending on the sample/tip distance. Prior to image acquisition, the tip is engaged from infinity distance onto the sample surface. As the tip comes closer to the surface, attractive van der Waals forces and dipol-dipol interactions begin to pull on it, causing the cantilever to bend (negative force). As the distance is lowered even further, a force minimum is reached, where the tip snaps into the

surface. After that point, the force rises exponentially and becomes positive as the tip is repelled from the sample surface.

The tip/sample distance (z-axis) is controlled by extremely precise and fast piezo actuators (voltage dependent expansion/shrinking ceramics). A laser beam is reflected from the back of the cantilever. Small changes in z-direction are greatly amplified due to the beam reflection angle change. Cantilever deflections that are even smaller than 10 nm can be detected by a multi-photometer. The great speed at which this can occur allows for great control over the applied forces. There are two more piezo elements in the x- and the y- dimension in order to allow full spatial control (rastering/scanning) over the AFM tip movement (Figure 51, right).

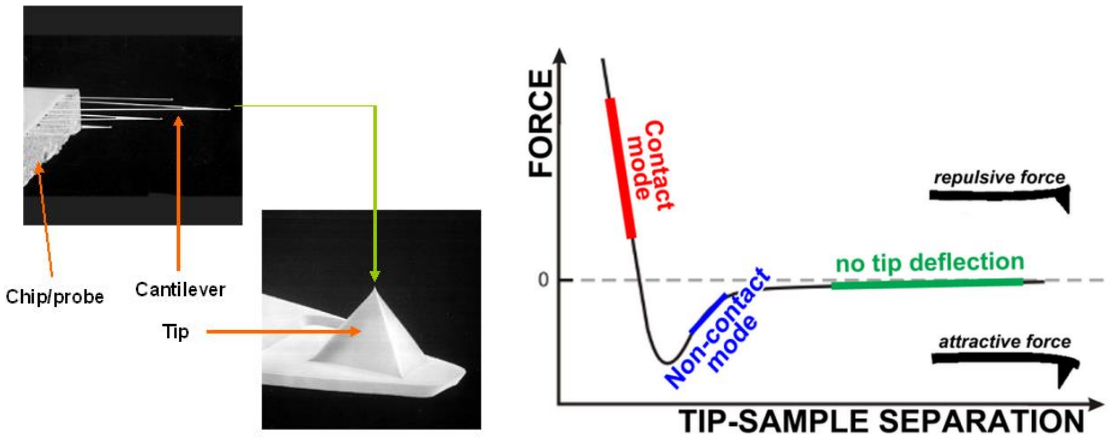

Figure 52: The AFM tip and its interaction with the sample surface. Left: SEM image of a chip with several cantilevers. Depending on the length and the geometry, the cantilevers have different spring constants (hardness). On the example of one case, the lower image shows a cantilever tip. In this case it consists of a sharpened pyramid (Bruker). Right: The Lennard-Jones-Potential on the right roughly displays the two different regions, of tip/sample interaction which contact and non-contact.

Measuring Modes: Depending on the tip/sample distance, the two modes non-contact and contact are defined (Figure 52, right). In between of those two extremes there is yet another intermittent mode called tapping mode (cf. **Figure 53**).

Contact Mode: In this mode, the cantilever tip comes directly in contact with the surface of the sample. This mode is recommended for stiff surfaces and on non-living samples as for example on a porous polyurethane membrane (cf. **Figure 54**). The cantilever is approached to the surface until the tip touches the surface. The laser beam is deviated by the bending of the cantilever. Then, the sample surface is scanned over the x- and y-axis and the z-piezo moves

in order to trace the topography of the sample. When the cantilever is in a depression area, the piezo is dilated. On a higher area the piezo retracts in order to keep the tip in contact with the surface. To obtain reproducible data, each line is measured twice: a trace and a retrace. If both lines are the same, the scanning parameters are optimal.

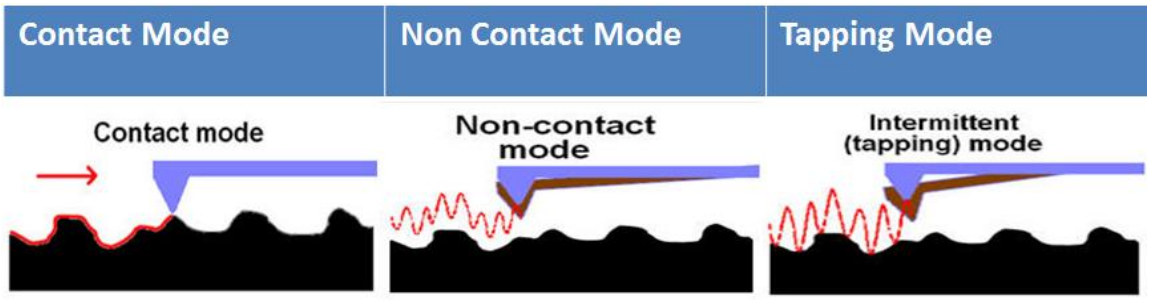

Figure 53: Schematic representation of the different AFM measuring modes.

Tapping Mode: In this mode, the cantilever comes in contact with the surface only at specific points. A current is applied to the piezo element based on the cantilever holder, which makes it oscillating at its harmonic frequency. The tip that oscillates with an amplitude of about 100 nm will touch the surface regularly. This technique is recommended for soft materials or living samples because it avoids the destruction or damage of the sample surface caused by forces generated in the contact mode.

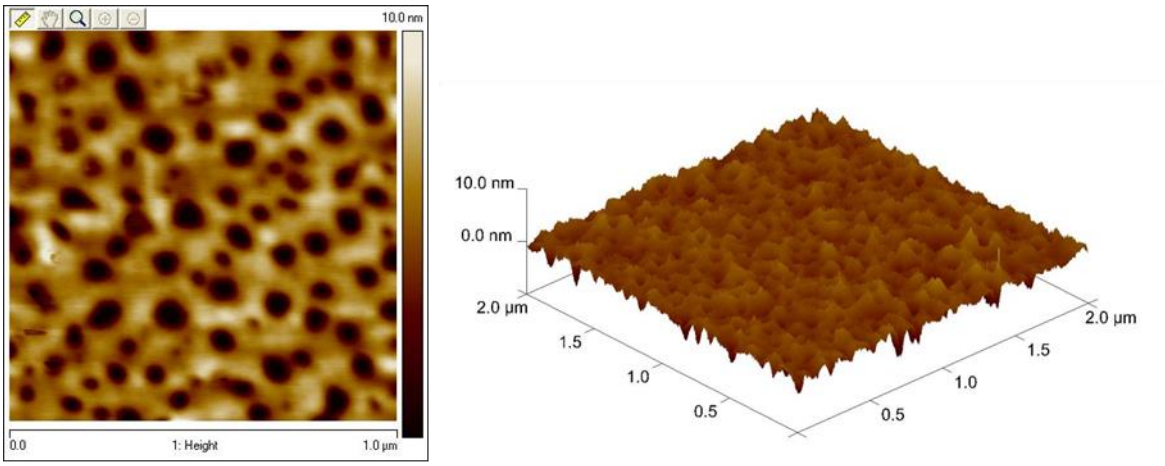

Figure 54: AFM images (contact mode) of porous polyurethane membranes. Left: height image. Right: 3D reconstruction. (Maziar Matloubi, Shastri Lab)

Tapping Mode with Phase Shift: Another feature of the intermittent mode is the possibility to characterize the homogeneity of a sample. The oscillation phase of the cantilever will shift as the surface underneath change. This allows the operator to resolve locations of different material compositions. Indeed, a change of the oscillation phase indicates that the tip "feel" a

smoother or stiffer area. This can be seen on the phase error images, where the areas of different compositions are then highlighted (cf. **Figure 55**).

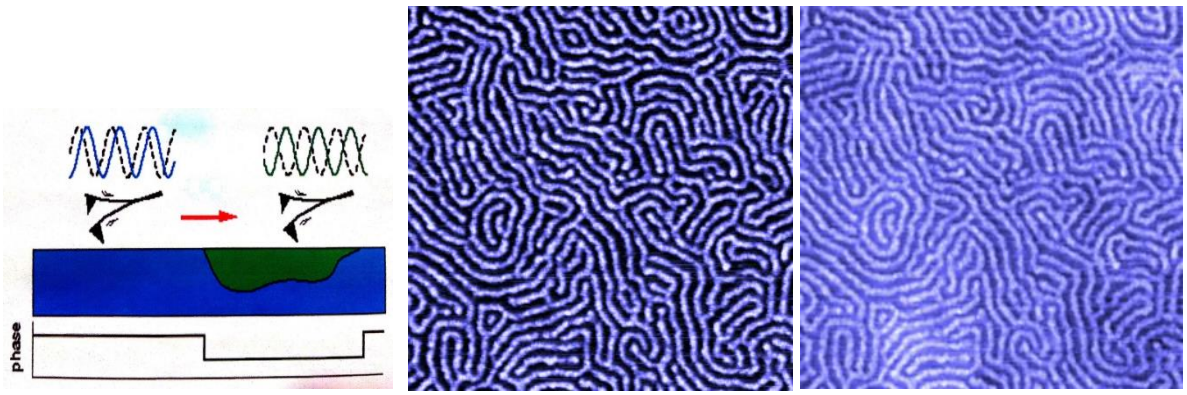

Figure 55: AFM (tapping mode) characterization of polystyrene-block-polybutadiene. Left: Scheme of the phase change depending on local differences in sample composition. Middle: Phase image. Right: height image.

All operations on the SEM, TEM and AFM will be done by trained staff. However the students will be involved in sample preparation and will be questioned on the basic principles as covered in this script.

Bibliography and Further Readings:

EM: http://www.explainthatstuff.com/electronmicroscopes.html

EM: http://cmrf.research.uiowa.edu/transmission-electron-microscopy

SEM: http://web.tiscali.it/barlini/affidabilita/sem/e_tesina/e_quartolink.htm

Bruker website : http://www.bruker-axs.com/atomicforcemicroscopy.html

IBM Zurich: http://www.zurich.ibm.com/

G. Binnig, C. F. Quate, and Ch. Gerber, *Phys. Rev. Lett*., **1986**, *56*, 930.

G. Binnig and D. P. E. Smith, *Rev. Sci. Instrum.,* **1986,** *57*, 1688.

Comprehensive book list on SEM, TEM, AFM:
http://www.tedpella.com/books_html/books.htm